This article has not been copyedited and formatted. The final version may differ from this version.
JPET Fast Forward. Published on August 21, 2013 as DOI: 10.1124/jpet.113.206623

JPET #206623

Title: *N*-aryl piperazine metabotropic glutamate receptor 5 positive allosteric modulators possess efficacy in pre-clinical models of NMDA hypofunction and cognitive enhancement

Authors: K.J. Gregory*, E.J. Herman*, A.J. Ramsey, A.S. Hammond, N.E. Byun, S.R. Stauffer, J.T. Manka, S. Jadhav, T.M. Bridges, C.D. Weaver, C.M. Niswender, T. Steckler, W.H. Drinkenburg, A. Ahnaou, H. Lavreysen, G.J. Macdonald, J.M. Bartolomé, C. Mackie, B.J. Hrupka, M.G. Caron, T.L. Daigle, C.W. Lindsley, P.J. Conn, C.K. Jones

Dept. Pharmacol. & Ctr. Neurosci. Drug Discov., Vanderbilt Univ., Nashville, TN, USA (KJG, EJH, ASH, NEB, SRS, JTM, SJ, TMB, CDW, CMN, CWL, PJC, CKJ); Drug Discovery Biology, MIPS, Monash University, Parkville, VIC, Australia (KJG); Dept. of Pharm. Toxicol., Univ. of Toronto, ON, Canada (AJR); Inst. Imaging Sci., Vanderbilt Univ., (NEB), Janssen Research and Development, a division of Janssen Pharmaceutica NV, Beerse, Belgium (TS, WHD, AA, HL, GJM, JMB, CM, BJH); Dept. Cell Biol., Duke University, Durham, NC, USA (TLD, MGC); Dept. Chem., Vanderbilt Univ. Med. Ctr., Nashville, TN, USA (CWL); U.S. Dept. of Veterans Affairs, Nashville, TN, USA (CKJ)

JPET Fast Forward. Published on August 21, 2013 as DOI: 10.1124/jpet.113.206623
This article has not been copyedited and formatted. The final version may differ from this version.

JPET #206623

Running Title: Pro-cognitive and antipsychotic efficacy of mGlu5 modulators

Corresponding Author:

Carrie K. Jones

Department of Pharmacology & Vanderbilt Center for Neuroscience Drug Discovery

Vanderbilt University Medical Center

Nashville, TN, USA

37232-0697

Telephone: 615-343-4337

Fax: 615-343-3088

Email: carrie.jones@vanderbilt.edu

Number of text pages: 63

Number of tables: 3

Number of figures: 14

Number of references: 65

Number of words in Abstract: 249

Number of words in Introduction: 582

Number of words in Discussion: 1574

Non-standard Abbreviations: 5-HT: serotonin; 5-MPEP: 5-methyl-2-(phenylethynyl)pyridine; ANOVA: analysis of variance; AW: active wakefulness; CDPPB: 3-cyano-*N*-(1,3-diphenyl-1*H*-pyrazol-5-yl)benzamide; CPPHA: *N*-[4-Chloro-2-[(1,3-dioxo-1,3-dihydro-2H-isoindol-2-yl)methyl]phenyl]-2-hydroxybenzamide; DA: dopamine; DMEM: Dulbecco's Modified Eagle's Medium; DMPK: drug metabolism and

JPET Fast Forward. Published on August 21, 2013 as DOI: 10.1124/jpet.113.206623
This article has not been copyedited and formatted. The final version may differ from this version.

pharmacokinetic; DMSO: dimethylsulfoxide; DPFE: 1-(4-(2,4-difluorophenyl)piperazin-1-yl)-2-((4-fluorobenzyl)oxy)ethanone; dSWS: deep non-REM/Slow Wave Sleep; EEG: electroencephalogram; EMG: electromyogram; EOG: electrooculogram; ERK1/2: extracellular signal-regulated kinases 1 and 2; FBS: fetal bovine serum; FFT: Fast Fourier Transform; GIRK: G protein-coupled inwardly-rectifying potassium channels; HPBCD: hydroxyl-propyl betacyclodextrin; IS: intermediate stage; lSWS: light non-REM/Slow Wave Sleep; LC/MS/MS: liquid chromatography with tandem mass spectrometry; mGlu: metabotropic glutamate receptor; MPEP: 2-methyl-6-(phenylethynyl)-pyridine; NAC: nucleus accumbens; NAM: negative allosteric modulator; NE: Norepinehrine; NMDA: N-methyl-D-aspartate; NMDAR: NMDA receptor; NR1KD: NR1 knockdown; PAM: positive allosteric modulator; pEEG: PharmacoEEG; pERK1/2: phosphorylated ERK1/2; PFC: prefrontal cortex; PPI: Prepulse Inhibition; PW: Passive Wakefulness; REM: paradoxical/Rapid Eye Movement Sleep; swEEG: Sleep/wake EEG; VU0364289: 2-(4-(2-(benzyloxy)acetyl)piperazin-1-yl)benzonitrile.

Section Assignment: Neuropharmacology

Abstract

Impaired transmission through glutamatergic circuits has been postulated to play a role in the underlying pathophysiology of schizophrenia. Furthermore, inhibition of *N*-methyl-D-aspartate (NMDA) subtype of ionotropic glutamate receptors (NMDAR) induces a syndrome that recapitulates many of the symptoms observed in schizophrenia patients. Selective activation of metabotropic glutamate receptor subtype 5 ($mGlu_5$) may provide a novel therapeutic approach for treatment of symptoms associated with schizophrenia through facilitation of transmission through central glutamergic circuits. Here, we describe the characterization of two novel N-aryl piperazine $mGlu_5$ positive allosteric modulators (PAMs), VU0364289, and 1-(4-(2,4-difluorophenyl)piperazin-1-yl)-2-((4-fluorobenzyl)oxy)ethanone (DPFE). VU0364289 and DPFE induced robust leftward shifts in the glutamate concentration-response curves for Ca^{2+} mobilization and ERK1/2 phosphorylation. Both PAMs displayed micromolar affinity for the common $mGlu_5$ allosteric binding site and high selectivity for $mGlu_5$. VU0364289 and DPFE possessed suitable pharmacokinetic properties for dosing in vivo and produced robust dose-related effects in reversing amphetamine-induced hyperlocomotion, a preclinical model predictive of antipsychotic-like activity. In addition, DPFE enhanced acquisition of contextual fear conditioning in rats and reversed behavioral deficits in a mouse model of NMDAR hypofunction. In contrast, DPFE had no effect on reversing apomorphine-induced disruptions of prepulse inhibition of the acoustic startle reflex. These $mGlu_5$ PAMs also increased monoamine levels in the prefrontal cortex, enhanced performance in a hippocampal mediated memory task, and elicited changes in EEG dynamics commensurate with pro-cognitive effects. Collectively, these data support and extend

JPET Fast Forward. Published on August 21, 2013 as DOI: 10.1124/jpet.113.206623
This article has not been copyedited and formatted. The final version may differ from this version.

the role for the development of novel $mGlu_5$ PAMs for the treatment of psychosis and cognitive deficits observed individuals with schizophrenia.

Introduction

Schizophrenia affects approximately 1% of the population worldwide and is characterized by three core symptom clusters, including positive symptoms, such as delusions and thought disorders; negative symptoms, including anhedonia and social withdrawal; and cognitive impairments (American Psychiatric Association, 2000). Poor functional and social outcomes are directly correlated with the cognitive deficits observed in patients with schizophrenia (Green, 2006; Wu et al., 2005). Currently available typical and atypical antipsychotic therapies are effective in decreasing the psychotic symptoms, but provide little or no relief for the negative symptoms or cognitive impairments and are associated with multiple adverse side effects (Adrianzen et al., 2010; Pramyothin and Khaodhiar, 2010; Swartz et al., 2008). Accumulating evidence suggests that impaired transmission through glutamatergic circuits may contribute to all three major symptom clusters observed in schizophrenia patients (Krystal et al., 2002; Lewis and Moghaddam, 2006). For example, selective antagonists of the *N*-methyl-D-aspartate (NMDA) subtype of glutamate receptor (NMDAR), such as phencyclidine (PCP), induce psychosis and cognitive impairments in humans comparable to the symptoms observed in schizophrenia (Javitt, 2007; Javitt and Zukin, 1991; Luby et al., 1959). Moreover, NMDAR antagonists or genetic knockdown of the NR1 subunit of the NMDAR results in a mouse model of NMDAR hypofunction, which displays locomotor hyperactivity, sensorimotor gating deficits, aberrant social interactions, spatial learning deficits (Ramsey, 2009). Numerous cellular, behavioral, and anatomical studies suggest that the metabotropic glutamate receptor subtype 5 ($mGlu_5$) is a closely associated signaling partner with the NMDAR and may provide critical regulation of

JPET Fast Forward. Published on August 21, 2013 as DOI: 10.1124/jpet.113.206623
This article has not been copyedited and formatted. The final version may differ from this version.

transmission through forebrain circuits that are thought to mediate the psychotomimetic effects of NMDAR antagonists (Herman et al., 2012). Based on this, it has been postulated that highly selective activators of $mGlu_5$ may provide a novel approach to treatment of schizophrenia that has potential for treatment of all major symptom clusters (positive, negative, and cognitive) of this disorder. While attempts to develop selective mGluR5 agonists have not been fruitful, there has been tremendous progress in discovery of highly selective positive allosteric modulators (PAMs) of mGluR5 These mGlu5 PAMs can influence the binding and/or function of the receptor when simultaneously occupied by an orthosteric ligand and offer a number of potential advantages over orthosteric agonists. PAMs that enhance receptor activity, but have no intrinsic efficacy, have the capacity to maintain the spatial and temporal aspects of synaptic transmission and enhance mGlu5-mediated synaptic plasticity without altering normal activity-dependence of specific forms of synaptic plasticity (Ayala et al., 2009; Noetzel et al., 2013). Furthermore, recent studies reveal that pure mGlu5 PAMs have clear advantages to mGlu5 agonists in terms of their safety profile (Rook et al., 2013). Several different $mGlu_5$ PAM chemotypes have been identified and previous studies have shown that $mGlu_5$ PAMs from different scaffolds exhibit efficacy in animal models predictive of antipsychotic-like and cognition-enhancing activity (Gastambide et al., 2012; Gastambide et al., 2013; Gilmour et al., 2013; Kinney et al., 2005; Liu et al., 2008b; Spear et al., 2011). Herein, we describe the in vitro and behavioral characterization of two *N*-aryl piperazine $mGlu_5$ PAMs; VU0364289, which was discovered in-house from an evolved high-throughput screening negative allosteric modulator (NAM) lead (Zhou et al., 2010), and DPFE (disclosed in a patent application

by Astra-Zeneca and NPS (WO 2007/087135)), both structural analogs of the recently published $mGlu_5$ PAM, CPPZ (Spear et al., 2011; Xiong et al., 2010). We found that these N-aryl piperazines were potent cooperativity-driven $mGlu_5$ PAMs with favorable pharmacokinetic and solubility properties for dosing in vivo and efficacious in preclinical models of NMDAR hypofunction, antipsychotic-like activity and cognition enhancement.

JPET Fast Forward. Published on August 21, 2013 as DOI: 10.1124/jpet.113.206623
This article has not been copyedited and formatted. The final version may differ from this version.

Methods

Materials. Dulbecco's Modified Eagle's Medium (DMEM), fetal bovine serum (FBS) and antibiotics were purchased from Invitrogen (Carlsbad, CA). [^{3}H]methoxyPEPy (76.3 Ci/mmol) was custom synthesized by PerkinElmer Life and Analytical Sciences (Waltham, MA). Unless otherwise stated, all other reagents were purchased from Sigma-Aldrich (St. Louis, MO) and were of an analytical grade.

Cell culture and receptor mutagenesis. Mutations were introduced into the wild type rat $mGlu_5$ in pCI:Neo using site-directed mutagenesis (Quikchange II, Agilent, Santa Clara, CA) and verified by sequencing. Wild type and mutant rat $mGlu_5$ receptor constructs were transfected into HEK293A cells, using Fugene6^{TM} (Promega, Madison, WI) as the transfection reagent. Polyclonal stable cell lines were derived for rat $mGlu_5$ mutant constructs by maintaining the cells at sub-confluence for a minimum of four passages in the presence of 1 mg/ml G418. Stably transfected cell lines were subsequently maintained in complete DMEM supplemented with 10% FBS, 2 mM L-glutamine, 20 mM HEPES, 0.1 mM Non-Essential Amino Acids, 1 mM sodium pyruvate, antibiotic-antimycotic and G418 (500 ug/ml; Mediatech, Manassas, VA) at 37°C in a humidified incubator containing 5% CO_2, 95% O_2. HEK293 cells stably expressing rat $mGlu_1$ were maintained in the same media as HEK293A-rat $mGlu_5$ cells. HEK293 cells stably expressing G protein-coupled inwardly-rectifying potassium channels (HEK293-GIRK) and each of the group II and group III mGlu's were maintained in growth media containing 45% DMEM, 45% F-12, 10% FBS, 20 mM HEPES, 2 mM L-glutamine, antibiotic/antimycotic, non-essential amino acids, 700 µg/ml G418, and 0.6 µg/ml puromycin.

JPET Fast Forward. Published on August 21, 2013 as DOI: 10.1124/jpet.113.206623
This article has not been copyedited and formatted. The final version may differ from this version.

Ca^{++} mobilization assays. The day prior to assay, HEK293A-rat $mGlu_5$ cells were seeded at 50,000 cells/well in poly-D-lysine coated black-walled, clear bottom 96 well plates in assay medium (DMEM supplemented with 10% dialyzed fetal bovine serum, 20 mM HEPES and 1 mM sodium pyruvate). The cell permeable Ca^{++} indicator dye Fluo-4 was used to assay receptor-mediated Ca^{++} mobilization as described previously (Hammond et al., 2010) using a Flexstation II (Molecular Devices, Sunnyvale, CA). A 5 point smoothing function was applied to the raw fluorescent Ca^{++} traces and basal fluorescence of individual wells determined during the first 20 sec. The increase in fluorescence over basal was determined for both peak and plateau phases of the response before being normalized to the maximal peak response elicited by glutamate.

ERK1/2 phosphorylation. Receptor-mediated extracellular signal-regulated kinases 1 and 2 (ERK1/2) phosphorylation was determined using the AlphaScreen™-based ERK SureFire™ kit (PerkinElmer Life and Analytical Sciences, Boston, MA & TGR Biosciences, Thebarton, Australia) as described previously (Gregory et al., 2012). Briefly, HEK293A-rat-$mGlu_5$ cells were plated at a density of 40,000 cells/well in clear 96 well poly-D-lysine coated plates in assay medium 16-24 hr prior to assay. Media was aspirated and cells washed once with serum-free media (DMEM supplemented with 16 mM HEPES) then serum starved for 6 hr prior to assay. Serum-free media was exchanged for fresh 20 min prior to exposure to modulators and/or glutamate at room temperature. For interaction experiments with allosteric modulators, cells were exposed to allosteric modulator or vehicle 1 min prior to stimulation with glutamate for 7 min. Assay was terminated by aspiration of ligand containing media and addition of 50 µl/well of Lysis buffer. Following agitation for 10 min, 4 µl of lysate was transferred to a white

JPET Fast Forward. Published on August 21, 2013 as DOI: 10.1124/jpet.113.206623
This article has not been copyedited and formatted. The final version may differ from this version.

384-well plate (Costar, Corning Life Sciences, Tewksbury, MA). Under light diminished conditions, 7 µl/well of Reaction buffer mixture (containing 1 part Activation buffer to 6 parts Reaction buffer and 1:250 (v/v) donor and acceptor beads) was added. After 90 min incubation at 37°C, AlphaScreen signal was measured using a H4 synergy reader (Biotek, Winooski, VT) with standard AlphaScreen settings. Data are expressed as fold increase over basal levels of phosphorylated ERK1/2 and/or normalized to the maximal response elicited by a glutamate.

Selectivity Screening

Rat mGlu$_1$. The day prior to assay, HEK293 cells stably expressing rat mGlu$_1$ were plated in black-walled, clear-bottomed, poly-D-lysine coated 384-well plates (Greiner Bio-One, Monroe, NC) in assay medium at a density of 20,000 cells/well. Assays were performed within Vanderbilt University's High-Throughput Screening Center as described previously (Hammond et al., 2010; Rodriguez et al., 2010). Ca^{++} flux was measured using the Functional Drug Screening System 6000 (FDSS6000, Hamamatsu, Japan); vehicle or test compound (10 µM) was added followed by a concentration response curve to glutamate. The change in relative fluorescence over basal was calculated before normalization to the maximal response to glutamate.

Group II and Group III mGlus. Compound activity at the group II and III mGlu's was assessed using thallium flux through GIRK channels as previously described (Hammond et al., 2010; Niswender et al., 2008). Briefly, the day prior to assay HEK293-GIRK cells expressing mGlu subtype 2, 3, 4, 6, 7 or 8 were plated into 384-well, black-walled, clear-bottom poly-D-lysine coated plates at a density of 15,000 cells/well in

JPET Fast Forward. Published on August 21, 2013 as DOI: 10.1124/jpet.113.206623
This article has not been copyedited and formatted. The final version may differ from this version.

assay medium. The following day, the medium was aspirated and replaced with assay buffer (Hank's Balanced Salt Solution, 20 mM HEPES, pH7.4) supplemented with 1 µM Fluozin2-AM (Invitrogen, Carlsbad, CA). For these assays, vehicle or test compound (10 µM) was added followed by a concentration response curve to glutamate (or L-AP4 in the case of $mGlu_7$) diluted in thallium buffer (125 mM $NaHCO_3$, 1 mM $MgSO_4$, 1.8 mM $CaSO_4$, 5 mM glucose, 12 mM thallium sulfate, 10 mM HEPES) and fluorescence measured using a FDSS 6000. Data were analyzed as described previously (Niswender et al., 2008).

Radioligand Binding assays – $mGlu_5$. Membranes were prepared from HEK293A cells expressing rat $mGlu_5$ and mutants thereof as follows. Cells were harvested by trypsinization and pelleted by centrifugation for 3 min at 300 x*g*. Cell pellets were re-suspended in ice-cold homogenization buffer (50 mM Tris-HCl, 10 mM EDTA, 0.9% NaCl, pH7.4), and homogenized by 3 x 10 sec bursts with a Tekmar TP-18/10S1 homogenizer (Tekmar, Cincinnati, OH) separated by 30 sec on ice. Cell fractions were separated by centrifugation at 1000 x*g* for 10 min. Supernatant was then centrifuged for 1 hr @ 30,000 x*g* and the resulting pellet re-suspended in ice-cold Ca^{++} assay buffer. For saturation binding experiments, membranes (20-50 µg/well) were incubated with a range of [^{3}H]methoxyPEPy concentrations (0.5 nM-60 nM) for 1 hr at room temperature with shaking in Binding Buffer (50 mM Tris-HCl, 0.9% NaCl, pH7.4). 10 µM MPEP was used to determine non-specific binding. For inhibition binding experiments, membranes were incubated with ~2 nM [^{3}H]methoxyPEPy and a range of concentrations of VU0364289 and DPFE (300 pM-100 µM) for 1 hr at room temperature with shaking in Ca^{++} assay with 1% DMSO final. Binding assays were terminated by rapid filtration

JPET Fast Forward. Published on August 21, 2013 as DOI: 10.1124/jpet.113.206623
This article has not been copyedited and formatted. The final version may differ from this version.

through GF/B Unifilter plates (PerkinElmer Life and Analytical Sciences, Boston, MA) using a Brandel 96-well plate Harvester (Brandel Inc., Gaithersburg, MD), and three washes with ice-cold Binding Buffer, separating bound from free radioligand. Plates were allowed to dry overnight prior to addition of MicroScint 20 (40 µl/well; PerkinElmer). Radioactivity was counted after at least 2 hr incubation using a TopCount Scintillation Counter (PerkinElmer Life and Analytical Sciences, Boston, MA).

Plasma protein binding. The protein binding of each compound was determined in human and rat plasma via equilibrium dialysis employing Single-Use RED Plates with inserts (ThermoFisher Scientific, Rochester, NY). Plasma (220 µL) was added to the 96 well plate containing test compound (5 µL) and mixed thoroughly. Subsequently, 200 µL of the plasma-compound mixture was transferred to the *cis* chamber (red) of the RED plate, with an accompanying 350 µL of phosphate buffer (25 mM, pH 7.4) in the *trans* chamber. The RED plate was sealed and incubated for 4 hr at 37°C with shaking. At completion, 50 µL aliquots from each chamber were diluted 1:1 (50 µL) with either plasma (*cis*) or buffer (*trans*) and transferred to a new 96 well plate, at which time ice-cold acetonitrile (2 volumes) was added to extract the matrices. The plate was centrifuged (3000 x*g* 10 min) and supernatants transferred and diluted 1:1 (supernatant: water) into a new 96 well plate, which was then sealed in preparation for LC/MS/MS analysis. Each compound was assayed in triplicate within the same 96-well plate.

In Vivo Studies

Subjects. Adult male Sprague-Dawley rats, weighing 250-275 g, (Harlan Laboratories, Indianapolis, IN) were used for pharmacokinetic, locomotor, pre-pulse inhibition,

JPET Fast Forward. Published on August 21, 2013 as DOI: 10.1124/jpet.113.206623
This article has not been copyedited and formatted. The final version may differ from this version.

contextual fear conditioning, and Irwin neurological studies and were approved by the Vanderbilt University Institutional Animal Care and Use Committee and conducted in accordance with the National Institutes of Health regulations of animal care covered in Principles of Laboratory Animal Care. In addition, adult male Sprague-Dawley rats (Harlan Laboratories, The Netherlands), weighing 250-300 g were used for the in vivo microdialysis and electroencephalography studies and were carried out in strict accordance with the European Communities Council Directive of 24th November 1986 (86/609/EEC) and were approved by the Animal Care and Use Committee of Janssen Research and Development, a division of Janssen Pharmaceutica NV and by the Local Ethical Committee. Food and water were available ad libitum for all animals. All rats were group-housed in a large colony room under a 12-h light-dark cycle with food and water available *ad libitum* unless otherwise under the specific behavioral test. For the majority of behavioral studies in rats and mice, we used a dose range between 10-100 mg/kg i.p. for both DPFE and VU0364289, which provided suitable pharmacokinetics for evaluation of these compounds in vivo; in the case of the translational approaches, such as the EEG studies, we evaluated the effects of these compounds after an oral route as would be used in a clinical setting. Finally, we choose to use substantially lower doses of DPFE to evaluate potential cognitive enhancing effects in the CFC study since higher doses decreased performance in this task.

In Vivo Pharmacokinetic Study. Rats treated with dose of either VU0364289 or DPFE (10 mg/kg, i.p.), then and trunk blood were collected at 0.25, 0.5, 1, 3, and 6 hr after euthanasia. Removed brains were thoroughly washed in saline and immediately frozen on dry ice and stored at -80°C. Plasma and brain homogenate samples were then

JPET Fast Forward. Published on August 21, 2013 as DOI: 10.1124/jpet.113.206623
This article has not been copyedited and formatted. The final version may differ from this version.

processed and subjected to LC/MS/MS analysis as described in detail previously (Noetzel et al., 2012).

Drugs. *D*-amphetamine hemisulfate, was obtained from Sigma-Aldrich (St. Louis, MO) and dissolved in double deionized water; risperidone was dissolved in acidified double deionized water; and VU0364289 and DPFE were dissolved 20% hydroxyl-propyl betacyclodextrin (HPBCD) in sterile water at 1 mg/ml. All solutions were adjusted to a pH of approximately 6-7 using 1N sodium hydroxide and administered in a volume of 1 mL/kg i.p. or 10 mL/kg p.o. for studies in rats and 10 mL/kg i.p. for studies in mice.

Amphetamine-Induced Hyperlocomotion. Amphetamine**-**induced hyperlocomotor activity studies were conducted using a SmartFrame Open Field System (KinderScientific, San Diego, CA) equipped with 32 horizontal (x- and y-axes) infrared photobeams located 1 cm above the floor of the chamber as previously described (Jones et al., 2008). Changes in ambulation or locomotor activity were measured as the number of total photobeam breaks, expressed in 5 min intervals and were recorded with a Pentium I computer equipped with the Motor Monitor System software (Kinder Scientific). Briefly, rats were habituated to the locomotor activity chambers for 30 min, then pretreated with either vehicle or dose of either VU0364289 or DPFE (10-100 mg/kg, i.p.). Thirty minutes later, rats were administered with either vehicle or amphetamine (1 mg/kg, subcutaneous, sc) and monitored for another 60 min.

Apomorphine-induced Disruption of Prepulse Inhibition (PPI) of the Acoustic Startle Reflex (ASR). Studies were conducted using startle chambers with a Plexiglas cylinder mounted on a piezoelectric accelerometer for detecting motion as previously

described (Jones et al., 2005). Following a 20 min pretreatment with vehicle, risperidone (3 mg/kg p.o.), or a dose of DPFE (30-100 mg/kg, p.o.), rats were injected with apomorphine (1mg/kg, s.c.), and after an additional 10 min, placed into individual startle chambers for the following paradigm. After a 5-min acclimation period, the rats were presented with five presentations of the startle stimulus alone, followed by seven randomized presentations of the following trial types: no stimulus, startle pulse alone (120 dB, 40-ms broadband noise burst), prepulse noise alone (82dB, 40-ms broadband noise burst), and three prepulse (72, 77, or 82 dB; 20 ms) plus startle pulse combinations. The intertrial interval varied pseudorandomly between 15 and 45 s and the interstimulus interval was 100 ms. Background noise of 67 dB was presented continuously. Percent PPI was calculated as 100* [(mean ASR - mean ASR in prepulse plus pulse trials)] / mean ASR in startle pulse trials].

Enhancement of Contextual Fear Conditioning (CFC). CFC studies were conducted in conditioning chambers housed in a sound-attenuating cubicle (Med Associates, St. Albans, VT) as previously described (Digby et al., 2012). All rats were handled and injected with saline for two days prior to conditioning. Rats were pretreated with DPFE (0-0.56 mg/kg i.p.) or vehicle 30 min before conditioning. The rats were placed in individual conditioning chambers and following a 2 min habituation period, one footshock (1-s, 0.5 mA) was delivered through the stainless steel grid floor, and after 45-s rats were returned to their homecage. After ~24 hr, the animals were exposed to the identical context for assessment of freezing behavior. All trials were video recorded (VID-CAM-MONO-2A, Med Associates) and scored blinded. The potential effect of DPFE on nociceptive response to the footshook stimulus was also separately

JPET Fast Forward. Published on August 21, 2013 as DOI: 10.1124/jpet.113.206623
This article has not been copyedited and formatted. The final version may differ from this version.

measured. Rats were pretreated with vehicle or DPFE (1 mg/kg i.p.) for 30 min, then placed in the conditioning chambers and behavioral changes in footshock threshold were assessed using increasing current from 0-0.5 mA in increments of 0.05mA.

***Nr1^{neo}* –/– Animals (NR1KD).** Since NMDAR antagonists are use-dependent channel blockers, we found that pretreatment or co-treatment of the $mGlu_5$ PAMs used in the present studies in combination with phencyclidine resulted in enhanced disruptive effects of PCP on the behavioral endpoints measured (i.e. increased PCP-induced hyperlocomotion). For this reason, we choose to evaluate the effects of our $mGlu_5$ PAMs in a genetic model of NMDR hypofunction in order to avoid confounds of observed when using use-dependent NMDAR channel blockers after acute challenge. NR1KD animals were generated as previously described (Mohn et al., 1999) to harbor a hypomorphic mutation of the Grin1 gene that encodes the NR1 subunit of NMDAR. This mutation has been previously shown to cause a 90% reduction in NR1 subunit levels in the homozygous state (Mohn et al., 1999). Heterozygous mutant mice were intercrossed to generate wild type (WT) and homozygous mutant (NR1KD) littermates on a genetically defined F1 background (C57Bl/6J:129X1Sv/J) as previously described (Ramsey et al., 2008).

Locomotor Activity. Mice were individually tested for motor activity at 10–14 weeks of age under standardized environmental conditions using an automated Omnitech Digiscan apparatus (AccuScan Instruments, Columbus, OH), in a 42 cm^2 plexiglass chamber. Changes in ambulation or locomotor activity were measured as the number of total photobeam breaks, expressed in 5 min intervals. Mice were pretreated for 30 min

with vehicle or dose of DPFE (30, 56.6 mg/kg, i.p.), then placed into locomotor activity chambers and monitored for 120 min.

Y maze Test. Mice were pretreated for 30 min with vehicle or dose of DPFE (10.0 mg/kg, i.p.), then placed in one arm of a standard Y-maze (San Diego Instruments) and allowed to navigate the maze for eight minutes with 20 LUX indirect lighting and monitored by video-based tracking software (Viewer2, Biobserve). Spontaneous alternations were recorded each time the mouse entered the three arms of the maze consecutively before re-entering an arm. The number of triplet entries (spontaneous alternation) was divided by the total number of arm entries to calculate the percent spontaneous alternation (%SAP).

Sociability Test. Sociability was measured using a modified method as previously described test (Moy et al., 2004). Mice were pretreated for 30 min with vehicle or DPFE (10.0 mg/kg, i.p.), then placed into a rectangular arena measuring 60 cm x 40.5 cm x 22 cm with 20 LUX indirect lighting. Within the arena, a novel gender and age-matched mouse was contained within an inverted wire cup so that the novel mouse was visible to the test mouse and could be accessed for sniffing and social investigation. Over a ten min testing period, the time (s) that the test mouse spent in social investigation within a 5 cm circular zone around the novel mouse was measured using video-based tracking software (Viewer2, Biobserve).

***In vivo microdialysis*.** Rats were singly housed, then surgically implanted with two guide cannula (CMA Microdialysis AB, Kista, Sweden); one into the left nucleus accumbens (NAC) (AP +1.7 mm bregma, ML 1.4 mm, DV 6.0 mm) and the other into

JPET Fast Forward. Published on August 21, 2013 as DOI: 10.1124/jpet.113.206623
This article has not been copyedited and formatted. The final version may differ from this version.

the right prefrontal cortex (PFC) (AP +2.75 mm, ML 0.75 mm, DV 0.75 mm) (Paxinos and Watson, 1998), and allowed to recover for 7 days. One day prior to testing, rats were transferred to the experimental room and inserted with microdialysis probes (PFC with 4 mm and NAC with 2 mm membrane length) containing a 20 Kd cut-off PAES membrane. Starting at 0700 h on the subsequent experimental day, dialysates were collected in 4 consecutive 30 min samples, followed by 8 consecutive 30 min samples post-administration of vehicle or dose of DPFE (10, 30 and 100 mg/kg, p.o.) in 20% HPBCD + Tween; n= 9-13 each treatment). Norepinehrine (NE), dopamine (DA) and serotonin (5-HT) levels were determined from brain dialysates by HPLC with a Waters Alliance HT 2795 system equipped with a Waters electrochemical detector W 2465. Chromatographic separation was achieved on an Atlantis (Waters) reversed-phase column (C18, 2.1mm IDx50mm, 3mm). The mobile phase was a mixture of acetonitrile (10%) and an aqueous solution (90%) of 60 mM sodium acetate, 0.1 mM EDTA and 2 mM DSA, pH adjusted to 5.8 by 100% acetic acid. The flow-rate was 1.0 mL/min. The capillary electrochemical cell was set at a potential 0.70 V and sensitivity of 1nA with filter at 0.1s. Data were analysed as the area under curve after vehicle or DPFE treatment.

Sleep/wake EEG study (swEEG). Rats were singly housed and maintained under controlled environmental conditions throughout: 22 ± 2°C ambient temperature, relative humidity 60%, 12:12 light cycle regime (lights on 12a.m, illumination intensity: ~100 lux). Rats were implanted with electroencephalogram (EEG) recording apparatus using the following method: under anesthesia, rats were placed in a stereotaxic apparatus and three small cavities drilled into the cranial bone without perforating the dura to receive 3

stainless steel fixing screw-electrodes (diameter 1 mm) for the polygraphic recording of frontal and parietal EEG; two electrodes were placed on each side of the sagittal suture (AP +2 mm, ML –2 mm; and AP –6 mm, ML +3 mm from the Bregma (Paxinos and Watson, 1998)), while the third (reference) electrode was positioned over the cerebellum. For recording the electrooculogram (EOG) and electromyogram (EMG), stainless steel wires (51/46 Teflon Bilaney, Germany) were placed in the periorbital and the nuchal muscle, respectively. All electrodes were fitted into an 8-hole connector and fixed with dental cement to the cranium. After a 10 day recovery period post-surgery, rats were given an additional 7 days habituation under home cage recording conditions before EEG data collection. Next, rats were connected with a rotating swivel to a bipolar recorder amplifier (Embla MedCare, Iceland) with an input range of ±500 mV. The frontal, parietal EEG, EOG and EMG signals and body movement activities were monitored for 20h, directly digitized at 2 kHz and subsequently managed by a software package (Somnologica Science, MedCare, Iceland).

Rats were pretreated with vehicle or dose of DPFE (10, 30, 100 mg/kg, p.o.), two EEG recording sessions were performed in 32 animals, randomly assigned to 4 treatment conditions (n=8, each treatment group). The first recording session started at 1330h and lasted 20 continuous hours after the administration of vehicle to all 32 rats. On 1330h the next day, the second recording session was performed for the same duration following administration of vehicle or dose of DPFE as outlined above. Off-line, sleep-wake staging was automatically executed for each 2 sec epoch and averaged for 30 min periods, based on 5 EEG frequency bandings (δ: 0.4-4 Hz, θ: 4.2-8 Hz, α: 8.2-12 Hz, σ: 12.2-14 Hz, β: 14.2-30 Hz), integrated EMG, EOG and body activity level. Each

JPET Fast Forward. Published on August 21, 2013 as DOI: 10.1124/jpet.113.206623
This article has not been copyedited and formatted. The final version may differ from this version.

EEG epoch was assigned one of six sleep stages, classified as being indicative of active wakefulness (AW), passive wakefulness (PW), light non-REM/Slow Wave Sleep (lSWS), deep non-REM/Slow Wave Sleep (dSWS), intermediate stage (IS) or paradoxical/Rapid Eye Movement sleep (REM). The amount of time spent in each vigilance state, the number and duration of episodes in each state, latencies for lSWS, dSWS and REM, and the number of shifts from one state to another one were calculated. Latency was defined as the time between the beginning of the recording and the appearance of the first sleep period lasting at least 30 sec. Time spent in each vigilance state (AW, PW, lSWS, dSWS, IS and REM) was expressed as a percentage of the recording period.

PharmacoEEG study. PharmacoEEG (pEEG) changes were determined in another group of rats under identical surgical and testing conditions as outlined under the sleep/wake EEG methods with the exception of the montage: pEEG animals were equipped with EEG and EMG electrodes as depicted in Supplementary Figure 1. PharmacoEEG recording was performed in the dark phase of the circadian time following pretreatment with vehicle or dose of DPFE (10, 30, 100 mg/kg, p.o.) (n=8 for each treatment group). A stable baseline EEG recording was collected for 30 min (animals were picked up and a marker is introduced to tag the start of baseline period), followed by the administration of vehicle or dose of DPFE with a second marker indicating the start of the pharmacological response and the subsequent 2h sampling period following the treatment. Continuous EEG and EMG field potentials were acquired at 2 kHz sample rate with an input range of +/- 500 mV through a Biosemi ActiveTwo system (Biosemi, Amsterdam, Netherlands) referenced to the CMS-DRL ground

(common mode reference for online data acquisition and impedance measures, which is a feedback loop driving the average potential across the montage close to the amplifier zero). The signals were amplified and analogue band-pass filtered between 1 and 100 Hz and digitized with 24-bit resolution.

Offline, the EEG power spectra were computed for consecutive 4s epochs in the frequency range of 0.5-100 Hz (Fast Fourier Transform (FFT) routine, Hanning window, 0.25 Hz resolution). Epochs with artifacts were discarded on the basis of automatic detection. Adjacent 0.25 Hz bins were summed into 1 Hz bins up to 100 Hz for the full power spectrum. The data between 48-52 Hz were removed due to 50 Hz artifacts. Absolute power spectra of EEG signals were also computed by integrating the power spectrum in the following frequency windows: δ band (1–4 Hz), θ band (θ1: 4–6.5 Hz, θ2: 6.5–8 Hz), α band (α1: 8-11; α2: 11-14 Hz), β band (14-32), γ band (γ1: 32-48; γ2: 52-100 Hz). Next, the spectral power values of consecutive 4s epochs were averaged and drug-induced changes in EEG oscillations were calculated in blocks of 15 min for 2h as the ratio of mean spectral power obtained following the administration of test drug versus the mean spectral power obtained during 30 min baseline period. This procedure allows for assessment of compound-induced changes in EEG power expressed at each frequency band as a percentage of the original power, compared to the vehicle condition.

Data Analysis. All computerized nonlinear regression was performed using Prism 5.01 (GraphPad Software, San Diego, CA). Agonist and PAM concentration-response curves were analyzed using either a three or four parameter-logistic equation as appropriate to determine estimates of potency (pEC_{50}) and maximal agonist effect (E_{max}).

JPET Fast Forward. Published on August 21, 2013 as DOI: 10.1124/jpet.113.206623
This article has not been copyedited and formatted. The final version may differ from this version.

Shifts of glutamate concentration-response curves by allosteric modulators were globally fitted to an operational model of allosterism (Leach et al., 2007):

$$Effect = \frac{E_m(\tau_A[A](K_B+\alpha\beta[B])+\tau_B[B]K_A)^n}{([A]K_B+K_AK_B+K_A[B]+\alpha[A][B])^n+(\tau_A[A](K_B+\alpha\beta[B])+\tau_B[B]K_A)^n} \quad \text{(equation 1)}$$

where A is the molar concentration of orthosteric agonist glutamate, B is the molar concentration of the allosteric modulator, K_A is the equilibrium dissociation constant of the orthosteric agonist, glutamate, and K_B is the allosteric modulator equilibrium dissociation constant. Affinity modulation is governed by the cooperativity factor α, and efficacy modulation is governed by β, where values of > 1 describe positive cooperativity, values < 1 (but greater the 0) denote negative cooperativity and values equal to 1 denote neutral cooperativity. The parameters τ_A and τ_B relate to the ability of the orthosteric and allosteric ligands, respectively, to engender receptor activation. E_m and *n* denote the maximal possible system response and the transducer function that links occupancy to response, respectively. Unless otherwise stated all parameters were derived from global fitting glutamate concentration-response curves in the absence and presence of allosteric modulators.

An alternative, simplified, version of this operational model was applied to estimate a composite cooperativity parameter (αβ) for PAMs (Leach et al., 2010):

$$y = basal + \frac{(E_m-basal)(\tau_A[A](K_B+\alpha\beta[B])+\tau_B[B]K_A)^n}{(\tau_A[A](K_B+\alpha\beta[B])+\tau_B[B]K_A)^n+(K_A(K_B+[B]))^n} \quad \text{(equation 2)}$$

where basal denotes the baseline level (ligand-independent) of the system response and all other parameters are as described above for equation 1.

To derive estimates of neutral ligand affinity from translocation of PAM concentration response curves, a competitive model (1) was applied as the Schild slope (*s*) was not significantly different to unity over the neutral allosteric ligand concentration range used:

JPET Fast Forward. Published on August 21, 2013 as DOI: 10.1124/jpet.113.206623
This article has not been copyedited and formatted. The final version may differ from this version.

$$y = bottom + \frac{top - bottom}{1 + 10^{\left[\log\left(EC_{50} \times \left[1 + \left(\frac{B}{10^{-pA_2}}\right)^{s}\right]\right) - A\right]}} \quad (3)$$

where *bottom* and *top* are the lower and upper plateaus, respectively, of the PAM concentration response curve, A is the molar concentration of PAM, B is the molar concentration of neutral modulator and EC_{50} is the molar concentration of PAM required to generate a response halfway between the *top* and *bottom*. pA_2 is the negative logarithm of the molar concentration of antagonist that requires a 2 fold higher concentration of PAM to achieve the same response. *s* is the Schild slope factor (Arunlakshana and Schild, 1959). If *s* was found to be not significantly different from 1 then it was constrained to equal 1 and the resulting pA_2 value is equal to the pK_B (the negative logarithm of the K_B).

Inhibition binding data sets were fitted to a one-site inhibition binding model and estimates of inhibitor dissociation constants (K_I) were derived using the Cheng-Prusoff equation (Cheng and Prusoff, 1973).

All affinity, cooperativity and potency parameters were estimated as logarithms and are expressed as the mean ± S.E.M. (Christopoulos, 1998). For all behavioral studies, statistical analyses were performed using one-way ANOVA or two-way ANOVA with a Dunnett's post-test and statistical significance was taken as $p < 0.05$. swEEG data was analyzed by a non-parametric analysis of variance of each 30min period, followed by a Wilcoxon-Mann-Whitney rank sum test of comparisons with the control group. Time course EEG spectral changes were submitted to two-way multivariate ANOVA for repeated measures with two main factors (treatment and period of recordings), followed by a one-way ANOVA with main factor treatment for each of the

15 min period. Plots for behavior studies were executed using SigmaPlot 11 (Systat Software, Inc. Chicago, IL USA) with statistical analyses performed using JMP version 8 (SAS Institute Inc., Cary, NC).

Results

Characterization of molecular pharmacology of N-aryl piperazine PAMs

We recently reported the discovery of VU0364289, an *N*-aryl piperazine $mGlu_5$ PAM, which evolved from derivatization of a high throughput screening $mGlu_5$ NAM lead (Zhou et al., 2010). First, we sought to definitively characterize the pharmacology of VU0364289 along with DPFE, a structural analog disclosed in a patent application by Astra-Zeneca (NPS WO 2007/087135) (Figure 1A). Exposure of HEK-293A cells stably expressing the rat $mGlu_5$ receptor to glutamate results in mobilization of intracellular Ca^{2+}, characterized by an initial transient peak followed by a sustained phase. Both DPFE and VU0364289 dose dependently potentiated the peak response (Figure 1B) and plateau phase (Supplementary Figure 2) of Ca^{2+} mobilization in response to glutamate. PAM concentration response curves performed in the presence of a low concentration of glutamate (~EC_{25}) yielded pEC_{50}'s of 6.92±0.15 (0.12 µM) and 6.35±0.12 (0.45 µM) for DPFE and VU0364289 respectively. Both compounds maximally potentiated the EC_{25} glutamate peak response and, in the absence of glutamate, partial agonism was observed at 30 µM and 100 µM only (Figure 1C). DPFE was assessed for its ability to enhance glutamate potency in both low- and high- $mGlu_5$ expressing cell lines (Figure 1D,E). In line with the data reported for VU0364289 (Gregory et al., 2012), in the low-expressing cell line, this interaction was characterized by a progressive leftward shift that approached a limit, with no change in the maximal response (Figure 1D). DPFE possessed a higher degree of cooperativity with glutamate than VU0364289, inducing 17.2±5.1 -fold compared to 7.3±0.1 -fold leftward shifts of the glutamate concentration response curve, respectively, at 30 µM. In the high

JPET Fast Forward. Published on August 21, 2013 as DOI: 10.1124/jpet.113.206623
This article has not been copyedited and formatted. The final version may differ from this version.

expressing HEK-$mGlu_5$ cell line, DPFE also increased the E_{max} of glutamate as well as inducing a similar degree of leftward shift of the glutamate concentration-response curve (Figure 1E). Analysis of these progressive fold-shift data utilizing an operational model of allosterism (Gregory et al., 2012; Leach et al., 2007) confirmed that DPFE has higher positive cooperativity (logβ) than VU0364289 (Table 1) and, similarly, low affinity for $mGlu_5$ (5 μM). Furthermore, in agreement with previous findings for VU0364289 among other $mGlu_5$ PAMs (Gregory et al., 2012), the assumption that affinity cooperativity was neutral (α=1) had no impact on modulator affinity or cooperativity estimation, suggesting that DPFE, like VU0364289, elicits its potentiation primarily via efficacy modulation (Table 1).

These *N*-aryl piperazines were also assessed in a second assay of $mGlu_5$ activation, namely, phosphorylation of ERK1/2 (pERK1/2). In the HEK293-$mGlu_5$ low expressing cell line, pERK1/2 levels transiently increase in response to glutamate, peaking at 7 min and returning to baseline levels by 15 min (Figure 2A). In contrast to the Ca^{2+} mobilization assay, at 3 μM, both VU0364289 and DPFE acted as agonists in inducing pERK1/2, displaying a similar time course to glutamate (Figure 2A). As agonists, both PAMs showed greater efficacy compared to glutamate with respect to pERK1/2 (Figure 2B). Commensurate with previous reports for VU0364289 (Gregory et al., 2012), DPFE also potentiates glutamate-induced pERK1/2, shifting the concentration-response curve to the left and increasing the E_{max} (Figure 2C). Application of the operational model of allosterism (equation 1) to these data reveals that, compared to the Ca^{2+} assay data, both VU0364289 and DPFE have higher affinity estimates and lower cooperativity values for pERK1/2 (Table 1).

JPET Fast Forward. Published on August 21, 2013 as DOI: 10.1124/jpet.113.206623
This article has not been copyedited and formatted. The final version may differ from this version.

N-aryl piperazine PAMs are competitive with the neutral allosteric ligand 5MPEP

Given that these PAMs are based on a structurally distinct chemical scaffold to those previously identified, we were interested in whether or not they interacted with the common allosteric site on $mGlu_5$ to which prototypical allosteric ligands, such as MPEP and the CDPPB series of PAMs, are known to bind. We first assessed the ability of the neutral allosteric ligand 5MPEP to shift the PAM concentration response curve in the presence of a low concentration of glutamate (Figure 3). 5MPEP alone had no effect on the response to glutamate; however, induced parallel rightward shifts of both VU0364289 (Figure 3A) and DPFE (Figure 3B) concentration response curves with no change in the E_{max}. This is consistent with a competitive mode of interaction between 5MPEP and these N-aryl piperazine PAMs. Furthermore, Schild regression of PAM EC_{50}'s in the absence and presence of 5MPEP yielded Schild slopes not significantly different from unity (Figure 3C). Direct application of a competitive model to these data gave similar affinity estimates for 5MPEP, pK_B = 6.17±0.11 (versus DPFE; 679 nM) and 6.10±0.11 (versus VU0364289; 802 nM), consistent with those previously reported (Rodriguez et al., 2005).

N-aryl piperazine PAMs interact with the common allosteric (MPEP-binding) site

As confirmation of a competitive mode of interaction with the common allosteric site of $mGlu_5$, the effect of two point mutations was examined on the ability of these PAMs to potentiate the response to glutamate (Figure 4A, 4C, 4E). In agreement with previous studies, substitution of Ala809 for Val (A809V) at the top of TM7 significantly reduces glutamate potentiation by VU29 (a CDPPB series PAM) and inhibition by MPEP (Figure

JPET Fast Forward. Published on August 21, 2013 as DOI: 10.1124/jpet.113.206623
This article has not been copyedited and formatted. The final version may differ from this version.

4B, Table 2). This mutation also abolished [^{3}H]methoxyPEPy specific binding up to 30 nM (data not shown). At A809V, potentiation of glutamate by 3 µM DPFE and VU0364289 was decreased 3-fold compared to wild type (Table 2). In TM1, F585I decreases potentiation by CPPHA but has no effect on PAMs interacting with the common allosteric "MPEP" site such as VU29 and the nicotinamide and picolinamide acetylenes ((Chen et al., 2007; Gregory et al., 2013; Gregory et al., 2012) Figure 4E, Table 2). Consistent with the hypothesis that these N-aryl piperazines interact with the common allosteric site, F585I had no effect on the ability of DPFE and VU0364289 to potentiate glutamate responses (Figure 4C).

These *N*-aryl piperazine PAMs were also investigated for their ability to inhibit [^{3}H]methoxyPEPy binding. In preliminary studies, VU0364289 did not fully displace [^{3}H]methoxyPEPy, with ~49% specific binding remaining at 30 µM (Stauffer et al., 2010); however, when conducted under different experimental conditions (in Ca^{++} assay buffer with 1% DMSO final), 25.4±2.5% specific binding remained in the presence of 100 µM VU0364289 (Gregory et al., 2012). Under these same conditions, 100 µM DPFE almost fully displaced the radioligand with only 9.7±1.2% specific binding remaining (Figure 5). Assuming a competitive interaction with [^{3}H]methoxyPEPy, the apparent affinity of DPFE, pK_i = 5.10±0.08 (K_i = 8 µM), agreed well with functional estimates from progressive fold-shift assays (Table 1).

DPFE and VU0364289 selectively potentiate activation of $mGlu_5$

Both of these *N*-aryl piperazine PAMs were also assessed for their ability to modulate glutamate activity of the other seven mGlu subtypes (preliminary data

JPET Fast Forward. Published on August 21, 2013 as DOI: 10.1124/jpet.113.206623
This article has not been copyedited and formatted. The final version may differ from this version.

reported for VU0364289 in (Zhou et al., 2010)). For all subtypes, the potential for modulation of the glutamate concentration response curve was assessed at 10 µM of either PAM, with the exception of $mGlu_7$, where L-AP4 was used as the agonist. Neither VU0364289 nor DPFE significantly modulated agonist activity at the other seven mGlu subtypes (Figure 6). To investigate their propensity to interact with other receptors and ion channels, these PAMs were also examined for their ability to inhibit radioligand binding at 68 other targets. At 10 µM, DPFE only displayed significant inhibition (~70%) at the σ_1 receptor. VU0364289, at 10 µM, only caused significant inhibition (~75%) at the $5\text{-}HT_{2B}$ receptor (Supplementary Figure 3).

Pharmacokinetic and behavioral toxicity profile of VU0364289 and DPFE

Table 2 summarizes the in vitro and in vivo pharmacokinetic parameters of VU0364289 and DPFE. Free fraction of a compound in the presence of plasma proteins and the stability of a compound in liver microsomes are important qualities in a desirable drug metabolism and pharmacokinetic (DMPK) profile. DPFE and VU0364289 were tested for plasma protein binding in the presence of rat plasma and were found to exhibit favorable free fraction with 96% and 90 bound, respectively. In tests for stability in rat and human liver microsomes, there was 26 and 58%, respectively, of parent compound remaining after 15 min incubation period with DPFE; similar experiments with VU0364289 using a 60 min incubation protocol (Zhou et al., 2010) revealed less than 5% of parent remaining in both rat and human liver microsomes. In vivo pharmacokinetic parameters of DPFE and VU0364289 were studied in rats following administration of 10 mg/kg i.p. in 20% HPBCD solution. At different time points, including 0.25, 0.5, 1, 3 and 6 hr after dosing, the concentrations of DPFE and

JPET Fast Forward. Published on August 21, 2013 as DOI: 10.1124/jpet.113.206623
This article has not been copyedited and formatted. The final version may differ from this version.

VU0364289 were measured in systemic plasma (trunk blood) and whole brain tissues. Both compounds were rapidly and significantly absorbed in rats as evident from systemic plasma concentrations (Figure 7A; 7B). The C_{max} of both compounds was achieved in systemic plasma within 0.25 hr of dosing with values of 1093 ng/ml (~3.0 µM) and 1280 ng/ml (~3.8 µM) for DPFE and VU0364289, respectively. Both compounds were characterized by excellent CNS penetration with AUC brain/AUC systemic plasma ratio of 1.26 for DPFE and 1.09 for VU0364289. Modified Irwin Neurological battery revealed little evidence of acute toxicity at 30 mg/kg and 56.6 mg/kg DPFE or 56.6 mg/kg VU0364289 (Supplementary Table 1).

DPFE and VU0364289 reverse amphetamine-induced hyperlocomotion

The ability of a compound to reverse amphetamine-induced hyperlocomotion in rodents, accomplished by both atypical and typical antipsychotics, is considered a predictive value of the antipsychotic efficacy of a compound (Kinney et al., 2003). Previous studies have established efficacy in this behavioral model for $mGlu_5$ PAMs (Kinney et al., 2005; Liu et al., 2008a; Liu et al., 2008b). Administration of 56.6 mg/kg and 100 mg/kg DPFE i.p. significantly reversed amphetamine-induced hyperlocomotion, with ~60% fewer ambulations observed, over the entire time course of the study (Figure 8A). This reversal was dose-dependent, with animals receiving 30 mg/kg DPFE i.p. in conjunction with s.c. amphetamine (1 mg/kg) showing significantly fewer ambulations than controls between the 80 and 95 min time points only. Administration of VU0364289 also dose-dependently reversed amphetamine-induced hyperlocomotor activity (Figure 8B). Animals receiving both the 56.6 mg/kg and 100 mg/kg doses of VU0364289 in

JPET Fast Forward. Published on August 21, 2013 as DOI: 10.1124/jpet.113.206623
This article has not been copyedited and formatted. The final version may differ from this version.

conjunction with amphetamine showed significantly fewer ambulations, achieving a similar level of reversal as DPFE.

DPFE does not reverse apomorphine-induced disruption of pre-pulse inhibition

The potential antipsychotic profile of DPFE was further profiled using pre-pulse inhibition (PPI) disrupted with apomorphine (Figure 9). As shown in Figure 9A, the atypical antipsychotic, risperidone (3 mg/kg), significantly reversed apomorphine-induced disruption of prepulse inhibition to the acoustic startle reflex at 10 decibels (db) and 15db. In comparison, DPFE (30-100 mg/kg, p.o.) did not significantly reverse apomorphine-induced disruption of PPI. Further, neither risperidone or DPFE influenced the apomorphine-induced decrease in startle amplitude (Figure 9B). These data provide a point of deviation from the preclinical profile reported for another $mGlu_5$ PAM, ADX47273 (Schlumberger et al., 2009). It is important to note that the oral route of administration may have reduced in vivo exposure to DPFE contributing to its lack of efficacy in this model.

***DPFE* enhances the acquisition of contextual fear conditioning**

Contextual fear conditioning is a form of Pavlovian classical conditioning that is mediated by the hippocampus (Phillips and LeDoux, 1992). As shown in Figure 10, pretreatment with DPFE (0.1-0.56 mg/kg, i.p.) produced dose-related enhancement in the acquisition of contextual fear conditioning, significant at the 0.56 mg/kg dose ($F_{3,17}$=4.95 $p<0.01$; * $p<0.01$). In a separate experiment, pretreatment with DPFE (1 mg/kg i.p.) had no effect on the threshold of sensitivity to the footshock stimulus as compared with vehicle treatment group (data not shown).

Investigation of DPFE efficacy in a rodent model of NMDA receptor hypofunction

Knockdown of the NR1 subunit of NMDAR in mice (NR1KD) provides a genetic model of NMDAR hypofunction. These mice have 10% of normal NMDA receptor function and display hyperlocomotor activity in comparison to wildtype mice (Mohn et al., 1999). Administration of 30 mg/kg DPFE significantly reduced ambulatory counts in transgenic mice compared with vehicle-treated NR1KD animals (Figure 11A). In addition, the number of ambulations of NR1KD mice receiving 56.6 mg/kg DPFE was significantly lower at all time points from 20-115 min, excluding the 45 min point. Further, wildtype animals treated with vehicle or DPFE were not significantly different at any time point. NR1KD mice also show impairments in working memory (y-maze; Figure 11B) and social interactions (Figure 11C). Compared to littermate controls, NR1KD mice travelled greater distance (12209±436 cm vs 8532±324 cm) and had increased arm entries (51.8±4.5 versus 28.7±0.9) during the course of the y-maze task. Administration of 10 mg/kg of DPFE slightly increased arm entries and distance travelled by both groups (wildtype: 40.9±3.2 entries, 10587±523 cm; NR1KD: 65.3±5.1 entries, 13286±407 cm), however this only reached significance for the wildtype animals. Cognitive performance in this task is assessed by the number of spontaneous alternations, treatment with 10 mg/kg of DPFE had no significant effect on y-maze performance. Social investigation by NR1KD mice and littermate controls was not influenced by administration of 10 mg/kg DPFE.

Effect of DPFE on neurotransmitter levels in key brain regions

Monoamine neurotransmitter levels were assessed in the nucleus accumbens (NAC) and prefrontal cortex (PFC) of male rats following dosing with DPFE using

microdialysis (Figure 12). Dose-dependent increases in PFC monoamine levels were observed. Administration of 10 mg/kg DPFE p.o. significantly increased PFC norepinephrine levels to 200% of control, while both 30 mg/kg and 100 mg/kg p.o. doses elevated norepinephrine, dopamine and serotonin levels to ~300-500% above baseline. These increases occurred in the first hour and were sustained up to 4 h post dosing with DPFE. In the NAC, norepinephrine and serotonin, but not dopamine, levels were also significantly increased (~300% over baseline levels), although only at the highest doses.

DPFE elicits changes in sleep/wake architecture and pEEG

Acute treatment with DPFE exerted several effects on the sleep-wake architecture of rats (Figure 13, line graphs). Most notably, administration of 30 mg/kg and 100 mg/kg of DPFE significantly and dose-dependently increased time spent in passive wakefulness during the first 4 h post administration (Figure 13, inset bar graphs). This increase in passive waking persisted throughout the light phase and for the highest dose protruded into the dark phase more than 10 h after administration at the expense of active waking: a significant increase in passive waking over the total recording time (20 h) was consequently also found after 30 mg/kg and 100 mg/kg as compared to vehicle treatment.

Furthermore, in the pEEG study dose-dependent effects DPFE were observed on θ1 and α1 oscillations as measured during the active (dark) phase (Figure 14). Higher frequencies, especially in the γ bands, were largely unaffected. Effects were most pronounced in the parietal and occipital areas as compared to more frontal areas

of the cortex (see Figure 14; frontal versus occipital comparison), where transduction of underlying hippocampal neuronal activity is less pronounced.

Discussion

The development of selective $mGlu_5$ PAMs has advanced as an important potential therapeutic strategy for the treatment of schizophrenia through the facilitation of forebrain glutamatergic signaling thought to be disrupted in this disorder. Herein, we described the in vitro and behavioral characterization of two *N*-aryl piperazine $mGlu_5$ PAMs, DPFE and VU0364289, both found to be selective, cooperativity-driven $mGlu_5$ PAMs that interact with the common MPEP allosteric site on $mGlu_5$. These *N*-aryl piperazines showed improved solubility and pharmacokinetic properties, efficacy in a preclinical model predictive of antipsychotic-like activity, and enhancement of dopamine release in the prefrontal cortex without producing behavioral toxicity. Moreover, DPFE enhanced acquisition of a hippocampal-mediated memory task and elicited changes in sleep/wake architecture consistent with a pro-cognitive pharmacologic profile. Finally, we provide the first report of reversal of behavioral deficits in NR1 KD mice, a genetic model of NMDAR hypofunction, using the $mGlu_5$ PAM DPFE. Collectively, these findings provide strong support for the hypothesis that selective $mGlu_5$ activation may serve as a novel approach for the treatment of psychotic symptoms and cognitive deficits in schizophrenic patients.

Rigorous pharmacological approaches were applied to probe the mechanism of action of DPFE and VU0364289. While DPFE and VU0364289 have similar affinity for $mGlu_5$, DPFE displays ~2 fold higher cooperativity, which is greater than several reported PAM scaffolds (Chen et al., 2008; Gilmour et al., 2013; Gregory et al., 2012; Hammond et al., 2010; Kinney et al., 2005; Liu et al., 2008b; Rodriguez et al., 2010; Vanejevs et al., 2008). In agreement with our recent findings, potentiation by these N-

JPET Fast Forward. Published on August 21, 2013 as DOI: 10.1124/jpet.113.206623
This article has not been copyedited and formatted. The final version may differ from this version.

aryl piperazine PAMs was attributable to a mechanism solely involving glutamate efficacy modulation. Furthermore, DPFE agonism for Ca^{2+} and pERK1/2 displayed a similarly biased agonist profile to that recently reported for other $mGlu_5$ agonist-PAMs (Gregory et al., 2012). The implications of these differences between $mGlu_5$ allosteric versus orthosteric agonism are yet to be determined. Given that DPFE and VU0364289 exhibit low affinity for $mGlu_5$ (≥8 μM), we conclude their pharmacological effect is largely driven via cooperativity.

Despite being from a distinct chemical scaffold, DPFE and VU0364289 interact with the common allosteric binding site on $mGlu_5$. Specifically, interactions with the neutral allosteric ligand 5MPEP were consistent with competition and potentiation by both PAMs was decreased at the A809V mutant receptor, a mutation known to impact "MPEP-site" modulators (Gregory et al., 2013). Both compounds also displaced [^{3}H]methoxyPEPy, although this was incomplete over the concentration range tested likely attributable to low compound affinity. Indeed, another PAM from this same scaffold, the lead compound (2b) (also referred to as CPPZ) with an ~3 fold higher affinity than DPFE, fully displaced [^{3}H]MPEP (Spear et al., 2011; Xiong et al., 2010). Together these data illustrate that the common $mGlu_5$ allosteric site can accommodate a diverse array of chemical scaffolds that show not only subtype selectivity but diverse pharmacology.

Both DPFE and VU0364289 produced robust dose-related reversals of amphetamine-induced hyperlocomotion, a preclinical model predictive of antipsychotic-like activity, consistent with a potential role for selective $mGlu_5$ PAMs in the treatment of the positive symptoms in schizophrenia. Our findings with DPFE and VU0364289

JPET Fast Forward. Published on August 21, 2013 as DOI: 10.1124/jpet.113.206623
This article has not been copyedited and formatted. The final version may differ from this version.

confirm and extend previous studies with earlier generation $mGlu_5$ PAMs, including CDPPB, ADX47273 and CPPZ (Kinney et al., 2005; Liu et al., 2008b; Rosenbrock et al., 2010; Schlumberger et al., 2009; Spear et al., 2011). In contrast, more recent studies using the $mGlu_5$ PAMs LSN2463359 and LSN2814617 reported only marginal antipsychotic-like effects (Gilmour et al., 2013). While the reasons for the apparent differences in antipsychotic-like activity across the different chemical classes of $mGlu_5$ PAMs are not well understood, there are clear differences at the molecular level in the actions of the *N*-aryl piperazine $mGlu_5$ PAMs relative to the LSN $mGlu_5$ PAMs. While both DPFE and VU0364289 are less potent than either LSN PAM, they have higher cooperativity with glutamate as evidenced by ≥10 fold leftward shift in the glutamate concentration response curve as compared with a 2-3 fold shift for LSN $mGlu_5$ PAMs (Gilmour et al., 2013). This cooperativity difference is also reflected in the PAM potency curves E_{max} values; potentiation by DPFE and VU0364289 reached the glutamate E_{max}, while LSN $mGlu_5$ PAMs achieved only 65-79%. Such differences suggest that the efficacy of DPFE and VU0364289 is cooperativity-driven in nature, whereas LSN $mGlu_5$ PAMs may rely more on affinity since previous studies reported a clear link between receptor occupancy and efficacy (Gilmour et al., 2013).

Activation of $mGlu_5$ directly potentiates NMDAR function and also has independent actions that increase excitatory transmission and synaptic plasticity in a manner similar to that of NMDAR activation in forebrain circuits (Herman et al., 2012). To date, most preclinical studies evaluating $mGlu_5$ PAMs efficacy on NMDAR hypofunction have focused primarily on pharmacological challenge models using different NMDAR antagonists. Unfortunately, these studies reported varying degrees of

JPET Fast Forward. Published on August 21, 2013 as DOI: 10.1124/jpet.113.206623
This article has not been copyedited and formatted. The final version may differ from this version.

efficacy in reversing the behavioral disruptions induced by different NMDAR antagonists, likely dependent on the antagonist mode-of-action (Gastambide et al., 2013; Gilmour et al., 2013; Liu et al., 2008b; Rosenbrock et al., 2010; Schlumberger et al., 2010). Thus, we evaluated the ability of DPFE to reverse the behavioral deficits in NR1KD mice, a genetic model of NMDAR hypofunction (Ramsey, 2009), to avoid potential confounds observed with NMDAR antagonist challenge models. NR1KD mice display an approximately 90% decrease in functional NMDARs in limbic and forebrain regions and corresponding behavioral alterations, including hyperlocomotor activity and performance deficits in social interaction and cognition (Dzirasa et al., 2009; Halene et al., 2009; Moy et al., 2012; Ramsey, 2009), comparable to those induced with NMDAR antagonists. Treatment with DPFE reversed the hyperlocomotor activity observed in the NR1KD mice similar to the effects observed with clinically available antipsychotics (Mohn et al., 1999). Sociability and performance deficits in Y maze memory task were not improved at the 10 mg/kg dose DPFE, suggesting higher doses may be required to normalize these cognitive deficits. Collectively, these data in the NR1KD mice provide independent validation for a role for selective $mGlu_5$ PAMs in reversing behavioral disruptions resulting from NMDAR hypofunction.

Interestingly, DPFE enhanced release of monoamines and serotonin in the PFC consistent with previously reported effects of the atypical antipsychotic risperidone (Gessa et al., 2000; Ohoyama et al., 2011). Importantly, increased extracellular DA and NE in the PFC are associated with the cognition-enhancing doses of methylphenidate and atomoxetine (Berridge et al., 2006; Bymaster et al., 2002). In contrast to the PFC effects, only 5-HT and NE levels were elevated in nucleus accumbens, DA levels were

JPET Fast Forward. Published on August 21, 2013 as DOI: 10.1124/jpet.113.206623
This article has not been copyedited and formatted. The final version may differ from this version.

unchanged. Prior in vivo microdialysis studies using $mGlu_5$ PAMs reported mixed outcomes in nucleus accumbens (e.g., ADX47273 (Liu et al., 2008b)), but no findings on PFC neurotransmitter changes. The lack of effect on extracellular levels of DA in the nucleus accumbens suggests a low potential for abuse liability with DPFE. In addition, both DPFE and VU0364289 were well tolerated after acute administration with a lack of acute toxicity in modified Irwin neurological test battery. To further understand the future utility of $mGlu_5$ PAMs in the clinic, it will also be important to evaluate the effects of DPFE and VU0364289 after repeated dosing. Here, we provide the first report of enhanced PFC monoamine levels induced by selective $mGlu_5$ enhancement, comparable in magnitude to clinically efficacious antipsychotics.

Facilitation of $mGlu_5$ plays a critical role in normal learning and memory functions, suggesting $mGlu_5$ PAMs may improve cognitive impairments associated with schizophrenia (Herman et al., 2012). While previous studies focused on $mGlu_5$ PAM reversal of psychostimulant-induced deficits in cognition (i.e.(Gastambide et al., 2013; Reichel et al., 2011)), we evaluated the ability of DPFE to facilitate the hippocampal-mediated acquisition of contextual fear conditioning, a classical Pavlovian conditioning task (Phillips and LeDoux, 1992). Interestingly, DPFE enhanced acquisition of this cognitive task within a dose range significantly lower than that required to reverse amphetamine-induced hyperlocomotion; consistent with the previous report of lower doses of the $mGlu_5$ PAM ADX47273 needed to enhance performance in another cognition model (Liu et al., 2008b). Further, DPFE dose-dependently elicited changes in rat sleep-wake architecture, primarily increasing passive wakefulness; mirroring the previous report that CDPPB increased wakefulness and light sleep, although no

JPET Fast Forward. Published on August 21, 2013 as DOI: 10.1124/jpet.113.206623
This article has not been copyedited and formatted. The final version may differ from this version.

distinction was made between active and passive wake (Parmentier-Batteur et al., 2012). Moreover, the novel $mGlu_5$ PAMs, LSN2463359 and LSN2814617 also increased wakefulness (Gilmour et al., 2013). A compensatory rebound in REM without a non-REM rebound was reported, indicating a lack of rebound hypersomnolence of $mGlu_5$ PAMs. This observation is in line with the present study design, which further differentiated between changes in light and deep non-REM sleep. Interestingly, the initial deep non-REM sleep reduction was accompanied by a light non-REM increase and slight deep non-REM compensation during the later hours of the 20 hr recording period. In the pharmacoEEG study, enhanced θ1 synchrony and decreased α1 synchrony was observed in response to acute dosing with DPFE. Increased θ rhythm in the PFC in response to several antipsychotics has been reported (Sebban et al., 1999). Clinically effective antipsychotics elicit decreases in α1 and γ2 EEG synchrony. It is noteworthy that DPFE, despite its antipsychotic profile, did not induce changes in γ2 EEG synchrony suggesting different potential mechanisms underlying the efficacy of $mGlu_5$ PAMs.

In summary, DPFE and VU0364289 represent an exciting structural class of selective and potent cooperativity-driven $mGlu_5$ PAMs with favorable pharmacokinetic properties and robust efficacy in several behavioral models at doses that did not produce adverse side effects as observed with other $mGlu_5$ activators. Our findings provide further support for $mGlu_5$ PAM development for the potential treatment of all three symptom clusters observed in individuals with schizophrenia.

Acknowledgements

The authors gratefully acknowledge the technical expertise of Kiran K. Gogi, Daryl F. Venable and Rocio Zamorano for performing the mGlu selectivity assays; Wendy Horsfall for assistance with behavioral tests on NR1 KD mice; Christ Nolten and Gerd Van Den Kieboom for support with microdialysis studies; Heidi Huysmans and Sofie Versweyveld for support with EEG studies.

Authorship Contributions

Participated in Research Design: Gregory, Herman, Jones, Drinkenburg, Mackie, Daigle, Caron, Weaver, Steckler, Lavreysen, Niswender, Jones, Conn

Conducted Experiments: Gregory, Herman, Hammond, Ramsey, Byun, Hrupka, Daigle, Jones, Jadhav, Bridges

Contributed new reagents or analytic tools: Lindsley, Stauffer, Bartolomé, Macdonald, Manka

Performed data analysis: Gregory, Herman, Ramsey, Ahnaou, Drinkenburg, Byun, Bridges, Daigle, Weaver, Jones, Lavreysen

Wrote or contributed to the writing of the manuscript: Gregory, Herman, Jones, Drinkenburg, Ramsey

Other: Sourced funds for the work: Conn, Lindsley, Ramsey, Caron.

References

Adrianzen C, Arango-Davila C, Araujo DM, Ruiz I, Walton RJ, Dossenbach M and Karagianis J (2010) Relative association of treatment-emergent adverse events with quality of life of patients with schizophrenia: post hoc analysis from a 3-year observational study. *Hum Psychopharmacol* **25**(6): 439-447.

American Psychiatric Association (2000) *Diagnostic and Statistical Manual of Mental Disorders*. 4th ed. American Psychiatric Publishing, Washington D.C.

Arunlakshana O and Schild HO (1959) Some quantitative uses of drug antagonists. *Br J Pharmacol Chemother* **14**(1): 48-58.

Ayala JE, Chen Y, Banko JL, Sheffler DJ, Williams R, Telk AN, Watson NL, Xiang Z, Zhang Y, Jones PJ, Lindsley CW, Olive MF and Conn PJ (2009) mGluR5 positive allosteric modulators facilitate both hippocampal LTP and LTD and enhance spatial learning. *Neuropsychopharmacology* **34**(9): 2057-2071.

Berridge CW, Devilbiss DM, Andrzejewski ME, Arnsten AF, Kelley AE, Schmeichel B, Hamilton C and Spencer RC (2006) Methylphenidate preferentially increases catecholamine neurotransmission within the prefrontal cortex at low doses that enhance cognitive function. *Biol Psychiatry* **60**(10): 1111-1120.

Bymaster FP, Felder C, Ahmed S and McKinzie D (2002) Muscarinic receptors as a target for drugs treating schizophrenia. *Curr Drug Targets CNS Neurol Disord* **1**(2): 163-181.

Chen Y, Goudet C, Pin JP and Conn PJ (2008) N-{4-Chloro-2-[(1,3-dioxo-1,3-dihydro-2H-isoindol-2-yl)methyl]phenyl}-2-hydroxybe nzamide (CPPHA) acts through a

novel site as a positive allosteric modulator of group 1 metabotropic glutamate receptors. *Mol Pharmacol* **73**(3): 909-918.

Chen Y, Nong Y, Goudet C, Hemstapat K, de Paulis T, Pin JP and Conn PJ (2007) Interaction of novel positive allosteric modulators of metabotropic glutamate receptor 5 with the negative allosteric antagonist site is required for potentiation of receptor responses. *Mol Pharmacol* **71**(5): 1389-1398.

Cheng Y and Prusoff WH (1973) Relationship between the inhibition constant (K1) and the concentration of inhibitor which causes 50 per cent inhibition (I50) of an enzymatic reaction. *Biochemical pharmacology* **22**(23): 3099-3108.

Christopoulos A (1998) Assessing the distribution of parameters in models of ligand-receptor interaction: to log or not to log. *Trends in pharmacological sciences* **19**(9): 351-357.

Digby GJ, Noetzel MJ, Bubser M, Utley TJ, Walker AG, Byun NE, Lebois EP, Xiang Z, Sheffler DJ, Cho HP, Davis AA, Nemirovsky NE, Mennenga SE, Camp BW, Bimonte-Nelson HA, Bode J, Italiano K, Morrison R, Daniels JS, Niswender CM, Olive MF, Lindsley CW, Jones CK and Conn PJ (2012) Novel allosteric agonists of M1 muscarinic acetylcholine receptors induce brain region-specific responses that correspond with behavioral effects in animal models. *J Neurosci* **32**(25): 8532-8544.

Dzirasa K, Ramsey AJ, Takahashi DY, Stapleton J, Potes JM, Williams JK, Gainetdinov RR, Sameshima K, Caron MG and Nicolelis MA (2009) Hyperdopaminergia and NMDA receptor hypofunction disrupt neural phase signaling. *J Neurosci* **29**(25): 8215-8224.

Gastambide F, Cotel MC, Gilmour G, O'Neill MJ, Robbins TW and Tricklebank MD (2012) Selective remediation of reversal learning deficits in the neurodevelopmental MAM model of schizophrenia by a novel mGlu5 positive allosteric modulator. *Neuropsychopharmacology* **37**(4): 1057-1066.

Gastambide F, Gilmour G, Robbins TW and Tricklebank MD (2013) The mGlu(5) positive allosteric modulator LSN2463359 differentially modulates motor, instrumental and cognitive effects of NMDA receptor antagonists in the rat. *Neuropharmacology* **64**: 240-247.

Gessa GL, Devoto P, Diana M, Flore G, Melis M and Pistis M (2000) Dissociation of haloperidol, clozapine, and olanzapine effects on electrical activity of mesocortical dopamine neurons and dopamine release in the prefrontal cortex. *Neuropsychopharmacology* **22**(6): 642-649.

Gilmour G, Broad LM, Wafford KA, Britton T, Colvin EM, Fivush A, Gastambide F, Getman B, Heinz BA, McCarthy AP, Prieto L, Shanks E, Smith JW, Taboada L, Edgar DM and Tricklebank MD (2013) In vitro characterisation of the novel positive allosteric modulators of the mGlu(5) receptor, LSN2463359 and LSN2814617, and their effects on sleep architecture and operant responding in the rat. *Neuropharmacology* **64**: 224-239.

Green MF (2006) Cognitive impairment and functional outcome in schizophrenia and bipolar disorder. *J Clin Psychiatry* **67**(10): e12.

Gregory KJ, Nguyen ED, Reiff SD, Squire EF, Stauffer SR, Lindsley CW, Meiler J and Conn PJ (2013) Probing the Metabotropic Glutamate Receptor 5 (mGlu5)

Positive Allosteric Modulator (PAM) Binding Pocket: Discovery of Point Mutations that Engender a "Molecular Switch" in PAM Pharmacology. *Mol Pharmacol*.

Gregory KJ, Noetzel MJ, Rook JM, Vinson PN, Stauffer SR, Rodriguez AL, Emmitte KA, Zhou Y, Chun AC, Felts AS, Chauder BA, Lindsley CW, Niswender CM and Conn PJ (2012) Investigating metabotropic glutamate receptor 5 allosteric modulator cooperativity, affinity, and agonism: enriching structure-function studies and structure-activity relationships. *Mol Pharmacol* **82**(5): 860-875.

Halene TB, Ehrlichman RS, Liang Y, Christian EP, Jonak GJ, Gur TL, Blendy JA, Dow HC, Brodkin ES, Schneider F, Gur RC and Siegel SJ (2009) Assessment of NMDA receptor NR1 subunit hypofunction in mice as a model for schizophrenia. *Genes Brain Behav* **8**(7): 661-675.

Hammond AS, Rodriguez AL, Townsend SD, Niswender CM, Gregory KJ, Lindsley CW and Conn PJ (2010) Discovery of a Novel Chemical Class of mGlu(5) Allosteric Ligands with Distinct Modes of Pharmacology. *ACS Chem Neurosci* **1**(10): 702-716.

Herman EJ, Bubser M, Conn PJ and Jones CK (2012) Metabotropic glutamate receptors for new treatments in schizophrenia. *Handb Exp Pharmacol*(213): 297-365.

Javitt DC (2007) Glutamate and schizophrenia: phencyclidine, N-methyl-D-aspartate receptors, and dopamine-glutamate interactions. *Int Rev Neurobiol* **78**: 69-108.

Javitt DC and Zukin SR (1991) Recent advances in the phencyclidine model of schizophrenia. *Am J Psychiatry* **148**(10): 1301-1308.

Jentsch JD, Tran A, Taylor JR and Roth RH (1998) Prefrontal cortical involvement in phencyclidine-induced activation of the mesolimbic dopamine system: behavioral and neurochemical evidence. *Psychopharmacology (Berl)* **138**(1): 89-95.

Jones CK, Brady AE, Davis AA, Xiang Z, Bubser M, Tantawy MN, Kane AS, Bridges TM, Kennedy JP, Bradley SR, Peterson TE, Ansari MS, Baldwin RM, Kessler RM, Deutch AY, Lah JJ, Levey AI, Lindsley CW and Conn PJ (2008) Novel selective allosteric activator of the M1 muscarinic acetylcholine receptor regulates amyloid processing and produces antipsychotic-like activity in rats. *J Neurosci* **28**(41): 10422-10433.

Jones CK, Eberle EL, Shaw DB, McKinzie DL and Shannon HE (2005) Pharmacologic interactions between the muscarinic cholinergic and dopaminergic systems in the modulation of prepulse inhibition in rats. *The Journal of pharmacology and experimental therapeutics* **312**(3): 1055-1063.

Kinney GG, Burno M, Campbell UC, Hernandez LM, Rodriguez D, Bristow LJ and Conn PJ (2003) Metabotropic glutamate subtype 5 receptors modulate locomotor activity and sensorimotor gating in rodents. *J Pharmacol Exp Ther* **306**(1): 116-123.

Kinney GG, O'Brien JA, Lemaire W, Burno M, Bickel DJ, Clements MK, Chen TB, Wisnoski DD, Lindsley CW, Tiller PR, Smith S, Jacobson MA, Sur C, Duggan ME, Pettibone DJ, Conn PJ and Williams DL, Jr. (2005) A novel selective positive allosteric modulator of metabotropic glutamate receptor subtype 5 has in vivo activity and antipsychotic-like effects in rat behavioral models. *J Pharmacol Exp Ther* **313**(1): 199-206.

Krystal JH, Anand A and Moghaddam B (2002) Effects of NMDA receptor antagonists: implications for the pathophysiology of schizophrenia. *Arch Gen Psychiatry* **59**(7): 663-664.

Leach K, Loiacono RE, Felder CC, McKinzie DL, Mogg A, Shaw DB, Sexton PM and Christopoulos A (2010) Molecular mechanisms of action and in vivo validation of an M4 muscarinic acetylcholine receptor allosteric modulator with potential antipsychotic properties. *Neuropsychopharmacology* **35**(4): 855-869.

Leach K, Sexton PM and Christopoulos A (2007) Allosteric GPCR modulators: taking advantage of permissive receptor pharmacology. *Trends in pharmacological sciences* **28**(8): 382-389.

Lewis DA and Moghaddam B (2006) Cognitive dysfunction in schizophrenia: convergence of gamma-aminobutyric acid and glutamate alterations. *Arch Neurol* **63**(10): 1372-1376.

Liu F, Grauer S, Kelley C, Navarra R, Graf R, Zhang G, Atkinson PJ, Popiolek M, Wantuch C, Khawaja X, Smith D, Olsen M, Kouranova E, Lai M, Pruthi F, Pulicicchio C, Day M, Gilbert A, Pausch MH, Brandon NJ, Beyer CE, Comery TA, Logue S, Rosenzweig-Lipson S and Marquis KL (2008a) ADX47273 [S-(4-fluoro-phenyl)-{3-[3-(4-fluoro-phenyl)-[1,2,4]-oxadiazol-5-yl]-piper idin-1-yl}-methanone]: a novel metabotropic glutamate receptor 5-selective positive allosteric modulator with preclinical antipsychotic-like and procognitive activities. *J Pharmacol Exp Ther* **327**(3): 827-839.

Liu F, Grauer S, Kelley C, Navarra R, Graf R, Zhang G, Atkinson PJ, Popiolek M, Wantuch C, Khawaja X, Smith D, Olsen M, Kouranova E, Lai M, Pruthi F,

Pulicicchio C, Day M, Gilbert A, Pausch MH, Brandon NJ, Beyer CE, Comery TA, Logue S, Rosenzweig-Lipson S and Marquis KL (2008b) ADX47273 [S-(4-fluoro-phenyl)-{3-[3-(4-fluoro-phenyl)-[1,2,4]-oxadiazol-5-yl]-piperidin-1- yl}-methanone]: a novel metabotropic glutamate receptor 5-selective positive allosteric modulator with preclinical antipsychotic-like and procognitive activities. *J Pharmacol Exp Ther* **327**(3): 827-839.

Luby ED, Cohen BD, Rosenbaum G, Gottlieb JS and Kelley R (1959) Study of a new schizophrenomimetic drug; sernyl. *AMA Arch Neurol Psychiatry* **81**(3): 363-369.

Mohn AR, Gainetdinov RR, Caron MG and Koller BH (1999) Mice with reduced NMDA receptor expression display behaviors related to schizophrenia. *Cell* **98**(4): 427-436.

Moy SS, Nadler JJ, Perez A, Barbaro RP, Johns JM, Magnuson TR, Piven J and Crawley JN (2004) Sociability and preference for social novelty in five inbred strains: an approach to assess autistic-like behavior in mice. *Genes Brain Behav* **3**(5): 287-302.

Moy SS, Nikolova VD, Riddick NV, Baker LK and Koller BH (2012) Preweaning sensorimotor deficits and adolescent hypersociability in Grin1 knockdown mice. *Dev Neurosci* **34**(2-3): 159-173.

Niswender CM, Johnson KA, Luo Q, Ayala JE, Kim C, Conn PJ and Weaver CD (2008) A novel assay of Gi/o-linked G protein-coupled receptor coupling to potassium channels provides new insights into the pharmacology of the group III metabotropic glutamate receptors. *Mol Pharmacol* **73**(4): 1213-1224.

Noetzel MJ, Gregory KJ, Vinson PN, Manka JT, Stauffer SR, Lindsley CW, Niswender CM, Xiang Z and Conn PJ (2013) A Novel Metabotropic Glutamate Receptor 5 Positive Allosteric Modulator Acts at a Unique Site and Confers Stimulus Bias to mGlu5 Signaling. *Mol Pharmacol* **83**(4): 835-847.

Noetzel MJ, Rook JM, Vinson PN, Cho HP, Days E, Zhou Y, Rodriguez AL, Lavreysen H, Stauffer SR, Niswender CM, Xiang Z, Daniels JS, Jones CK, Lindsley CW, Weaver CD and Conn PJ (2012) Functional impact of allosteric agonist activity of selective positive allosteric modulators of metabotropic glutamate receptor subtype 5 in regulating central nervous system function. *Mol Pharmacol* **81**(2): 120-133.

Ohoyama K, Yamamura S, Hamaguchi T, Nakagawa M, Motomura E, Shiroyama T, Tanii H and Okada M (2011) Effect of novel atypical antipsychotic, blonanserin, on extracellular neurotransmitter level in rat prefrontal cortex. *European journal of pharmacology* **653**(1-3): 47-57.

Parmentier-Batteur S, O'Brien JA, Doran S, Nguyen SJ, Flick RB, Uslaner JM, Chen H, Finger EN, Williams TM, Jacobson MA and Hutson PH (2012) Differential effects of the mGluR5 positive allosteric modulator CDPPB in the cortex and striatum following repeated administration. *Neuropharmacology* **62**(3): 1453-1460.

Paxinos G and Watson C (1998) *The Rat Brain in Stereotaxic Coordinates*. 4th Edition ed. Academic Press.

Phillips RG and LeDoux JE (1992) Differential contribution of amygdala and hippocampus to cued and contextual fear conditioning. *Behav Neurosci* **106**(2): 274-285.

Pramyothin P and Khaodhiar L (2010) Metabolic syndrome with the atypical antipsychotics. *Curr Opin Endocrinol Diabetes Obes* **17**(5): 460-466.

Ramsey AJ (2009) NR1 knockdown mice as a representative model of the glutamate hypothesis of schizophrenia. *Prog Brain Res* **179**: 51-58.

Ramsey AJ, Laakso A, Cyr M, Sotnikova TD, Salahpour A, Medvedev IO, Dykstra LA, Gainetdinov RR and Caron MG (2008) Genetic NMDA receptor deficiency disrupts acute and chronic effects of cocaine but not amphetamine. *Neuropsychopharmacology* **33**(11): 2701-2714.

Reichel CM, Schwendt M, McGinty JF, Olive MF and See RE (2011) Loss of object recognition memory produced by extended access to methamphetamine self-administration is reversed by positive allosteric modulation of metabotropic glutamate receptor 5. *Neuropsychopharmacology* **36**(4): 782-792.

Rodriguez AL, Grier MD, Jones CK, Herman EJ, Kane AS, Smith RL, Williams R, Zhou Y, Marlo JE, Days EL, Blatt TN, Jadhav S, Menon UN, Vinson PN, Rook JM, Stauffer SR, Niswender CM, Lindsley CW, Weaver CD and Conn PJ (2010) Discovery of novel allosteric modulators of metabotropic glutamate receptor subtype 5 reveals chemical and functional diversity and in vivo activity in rat behavioral models of anxiolytic and antipsychotic activity. *Mol Pharmacol* **78**(6): 1105-1123.

Rodriguez AL, Nong Y, Sekaran NK, Alagille D, Tamagnan GD and Conn PJ (2005) A close structural analog of 2-methyl-6-(phenylethynyl)-pyridine acts as a neutral allosteric site ligand on metabotropic glutamate receptor subtype 5 and blocks the effects of multiple allosteric modulators. *Mol Pharmacol* **68**(6): 1793-1802.

Rodriguez AL, Zhou Y, Williams R, David Weaver C, Vinson PN, Dawson ES, Steckler T, Lavreysen H, Mackie C, Bartolome JM, Macdonald GJ, Scott Daniels J, Niswender CM, Jones CK, Jeffrey Conn P, Lindsley CW and Stauffer SR (2012) Discovery and SAR of a novel series of non-MPEP site mGlu(5) PAMs based on an aryl glycine sulfonamide scaffold. *Bioorg Med Chem Lett* **22**(24): 7388-7392.

Rook JM, Noetzel MJ, Pouliot WA, Bridges TM, Vinson PN, Cho HP, Zhou Y, Gogliotti RD, Manka JT, Gregory KJ, Stauffer SR, Dudek FE, Xiang Z, Niswender CM, Daniels JS, Jones CK, Lindsley CW and Conn PJ (2013) Unique signaling profiles of positive allosteric modulators of metabotropic glutamate receptor subtype 5 determine differences in in vivo activity. *Biol Psychiatry* **73**(6): 501-509.

Rosenbrock H, Kramer G, Hobson S, Koros E, Grundl M, Grauert M, Reymann KG and Schroder UH (2010) Functional interaction of metabotropic glutamate receptor 5 and NMDA-receptor by a metabotropic glutamate receptor 5 positive allosteric modulator. *European journal of pharmacology* **639**(1-3): 40-46.

Schlumberger C, Pietraszek M, Gravius A and Danysz W (2010) Effects of a positive allosteric modulator of mGluR5 ADX47273 on conditioned avoidance response and PCP-induced hyperlocomotion in the rat as models for schizophrenia. *Pharmacol Biochem Behav* **95**(1): 23-30.

Schlumberger C, Pietraszek M, Gravius A, Klein KU, Greco S, More L and Danysz W (2009) Comparison of the mGlu(5) receptor positive allosteric modulator ADX47273 and the mGlu(2/3) receptor agonist LY354740 in tests for antipsychotic-like activity. *European journal of pharmacology* **623**(1-3): 73-83.

Sebban C, Tesolin-Decros B, Millan MJ and Spedding M (1999) Contrasting EEG profiles elicited by antipsychotic agents in the prefrontal cortex of the conscious rat: antagonism of the effects of clozapine by modafinil. *Br J Pharmacol* **128**(5): 1055-1063.

Spear N, Gadient RA, Wilkins DE, Do M, Smith JS, Zeller KL, Schroeder P, Zhang M, Arora J and Chhajlani V (2011) Preclinical profile of a novel metabotropic glutamate receptor 5 positive allosteric modulator. *Eur J Pharmacol* **659**(2-3): 146-154.

Swartz MS, Stroup TS, McEvoy JP, Davis SM, Rosenheck RA, Keefe RS, Hsiao JK and Lieberman JA (2008) What CATIE found: results from the schizophrenia trial. *Psychiatr Serv* **59**(5): 500-506.

Vanejevs M, Jatzke C, Renner S, Muller S, Hechenberger M, Bauer T, Klochkova A, Pyatkin I, Kazyulkin D, Aksenova E, Shulepin S, Timonina O, Haasis A, Gutcaits A, Parsons CG, Kauss V and Weil T (2008) Positive and negative modulation of group I metabotropic glutamate receptors. *J Med Chem* **51**(3): 634-647.

Wu EQ, Birnbaum HG, Shi L, Ball DE, Kessler RC, Moulis M and Aggarwal J (2005) The economic burden of schizophrenia in the United States in 2002. *J Clin Psychiatry* **66**(9): 1122-1129.

Xiong H, Brugel TA, Balestra M, Brown DG, Brush KA, Hightower C, Hinkley L, Hoesch V, Kang J, Koether GM, McCauley JP, Jr., McLaren FM, Panko LM, Simpson TR, Smith RW, Woods JM, Brockel B, Chhajlani V, Gadient RA, Spear N, Sygowski LA, Zhang M, Arora J, Breysse N, Wilson JM, Isaac M, Slassi A and King MM

(2010) 4-aryl piperazine and piperidine amides as novel mGluR5 positive allosteric modulators. *Bioorg Med Chem Lett* **20**(24): 7381-7384.

Zhang Y, Rodriguez AL and Conn PJ (2005) Allosteric potentiators of metabotropic glutamate receptor subtype 5 have differential effects on different signaling pathways in cortical astrocytes. *The Journal of pharmacology and experimental therapeutics* **315**(3): 1212-1219.

Zhou Y, Manka JT, Rodriguez AL, Weaver CD, Days EL, Vinson PN, Jadhav S, Hermann EJ, Jones CK, Conn PJ, Lindsley CW and Stauffer SR (2010) Discovery of N-Aryl Piperazines as Selective mGluR5 Potentiators with Improved In Vivo Utility. *ACS Medicinal Chemistry Letters* **1**(8): 433-438.

Footnotes:

This work was supported by the National Institute of Health National Institute of Mental Health [R01 MH062646, R01 MH073853]; National Institute on Drug Abuse [F32 DA 030026]; National Institute of Neurological Disorders and Stroke [5R01 NS031373-15] and from an industry sponsored contract from Johnson & Johnson. Dr. Karen J. Gregory is supported by a National Health and Medical Research Council (Australia) Overseas Biomedical Postdoctoral Training fellowship; American Australian Association Merck Co. foundation fellowship and NARSAD-Maltz Investigator award. Work in Dr. Amy J. Ramsey's laboratory is supported by a Canadian Institutes of Health operating grant [258294].

* these authors contributed equally to this work

Legend for figures:

Figure 1 Potentiation of glu mediated Ca^{++} mobilization by *N*-aryl piperazines

A) Chemical structures of VU0364289 and DPFE. Changes in intracellular Ca^{++} mobilization following exposure to modulators in the absence and presence of glutamate were investigated in HEK293A cells stably expressing rat $mGlu_5$ using a Fluo-4 fluorescence-based Ca^{++} assay. B) Concentration-response curves for VU0364289 and DPFE to a low dose of glutamate (sub-EC_{30}) are shown. C) Response to VU0364289 and DPFE in absence of glu; concentration response curve to glutamate is shown (closed squares) for reference. HEK293A cells stably expressing rat $mGlu_5$, at relatively low (D) and high (E) levels were exposed to different concentrations of DPFE (as indicated below figure) for 60 sec prior to generation of a glutamate concentration-response curve for intracellular Ca^{++} mobilization. Data represent the mean ± s.e.m. of 4-8 independent experiments performed in duplicate. Error bars not shown lie within the dimensions of the symbol.

Figure 2 mGlu5 PAMs potentiate glu- mediated pERK1/2 and show robust agonist activity.

In HEK293A cells expressing low levels of $mGlu_5$, 1mM glutamate, 3 µM DPFE or 3 µM VU0364289 transiently increase levels of phosphorylated ERK1/2, peaking at 7-8 min and returning to baseline by 15 min (A), whilst vehicle has no effect. Concentration response-curves (B) reveal DPFE and VU0364289 are more efficacious agonists than glutamate. C) Increasing concentrations of DPFE raise baseline levels of pERK1/2 and shift the glutamate concentration-response curve to the left. Data represent the mean ±

s.e.m. of 3-6 independent experiments performed in triplicate. Error bars not shown lie within the dimensions of the symbol.

Figure 3 5MPEP inhibition of *N*-aryl piperazine potentiation of glutamate

HEK293A cells stably expressing rat $mGlu_5$ were exposed to different concentrations of 5MPEP for 60 sec prior to addition of a concentration range of PAM followed by addition of a low dose of glutamate (sub-EC_{30}). Rightward shifts in potentiator concentration-response curves (A & B) caused by co-addition of 5MPEP. C) Schild regression of changes in VU0364289 (closed circles) and DPFE (open circles) concentration-response curve EC_{50}'s in presence of 5MPEP. Data represent the mean ± s.e.m. of 4-6 independent experiments performed in duplicate. Error bars not shown lie within the dimensions of the symbol.

Figure 4 Effect of point mutations on $mGlu_5$ allosteric modulators

Polyclonal HEK293A cells stably expressing rat $mGlu_5$ wild type and mutant constructs were exposed to a single concentration of allosteric modulator prior to generation of concentration-response curves for glutamate-mediated Ca^{++} mobilization. A & B) glutamate concentration-response curve at the wild type receptor in the absence and presence of modulators. C & D) glutamate concentration-response curve at $mGlu_5$-A809V in the absence and presence of modulators. E & F) glutamate concentration-response curve at $mGlu_5$-F585I in the absence and presence of modulators. In all panels the concentration-response curve for glutamate in the absence of modulator is shown in closed circles, in the presence of 3 μM VU0364289 (closed squares, 3 μM

DPFE (open squares), 3 μM CPPHA (closed triangles), 3 μM VU29 (open triangles) and 10 nM MPEP (open circles). Data represent the mean ± s.e.m. of 4-8 independent experiments performed in duplicate. Error bars not shown lie within the dimensions of the symbol.

Figure 5 Inhibition of [^{3}H]methoxyPEPy binding by N-aryl piperazines in comparison to MPEP

Membranes prepared from HEK293A cells stably expressing rat $mGlu_5$ were incubated with 1-3nM [^{3}H]methoxyPEPy in the absence and presence of a range of concentrations of MPEP, VU0364289 or DPFE for 1 hr at room temperature. VU0364289 and MPEP data previously reported in Gregory et al., 2012 and is provided for reference. Data represent the mean ± s.e.m. of 3-4 independent experiments performed in triplicate. Error bars not shown lie within the dimensions of the symbol.

Figure 6 Selectivity of *N*-aryl piperazines across other mGlu subtypes

A single concentration (10 μM) of VU0364289 (closed squares) and DPFE (open squares) was assessed for modulation of orthosteric agonist activity (closed circles) (glutamate at all except $mGlu_7$ where L-AP4 was used) across the other seven mGlu subtypes. Activity at $mGlu_1$ was investigated using fluo-4 fluoresence-based measurement of Ca^{++} mobilization. Activity at all other subtypes was assessed by a fluorescence-based assay of thallium-flux through GIRK channels (Niswender et al., 2008). Data represent the mean ± s.e.m. of 3 independent experiments performed in

triplicate, with the exception of $mGlu_1$ where the mean of 2 independent experiments are shown. Error bars not shown lie within the dimensions of the symbol.

Figure 7 In vivo pharmacokinetic profile of VU0364289 (panel A) and DPFE (panel B)

Data represent mean determinations from 2 animals.

Figure 8 VU0364289 and DPFE dose-dependently reversed amphetamine-induced hyperlocomotion

Rats were placed in the open-field chambers for 30 min habituation interval, prior to pretreatment with vehicle or indicated dose of test compound in 20% HPBCD vehicle i.p. for an additional 30 min. All rats then received an injection of 1 mg/kg s.c. amphetamine, and locomotor activity was measured for an additional 60 min. A) VU0364289 produced a significant dose-dependent reversal of amphetamine-induced hyperlocomotion when administered i.p. and had no effect when administered alone. B) DPFE produced a significant reversal of amphetamine-induced hyperlocomotion and had no effect when administered alone. Data are expressed as mean ± s.e.m. of the number of beam breaks/ 5 min; error bars not shown lie within the dimensions of the symbol (n = 8-14 per dose). *, $p<0.05$ vs. vehicle + amphetamine, Dunnett's test.

Figure 9 DPFE does not reverse apomorphine-induced disruption of prepulse inhibition

A) The effect of DPFE (30 mg/kg, 56.6 mg/kg, 100 mg/kg) on apomorphine-induced disruption of prepulse inhibition of the acoustic startle reflex was assessed in rats in

parallel with the positive control risperidone (3 mg/kg). Data are expressed as changes in the % inhibition. B) The startle amplitude was not significantly different for any of the treatment groups. Bars represent the mean ± s.e.m value for 6-7 rats per dose group. * $p \leq 0.05$ vs. Vehicle/Apomorphine group, Dunnett's test.

Figure 10 DPFE Enhances Acquisition of Contextual Fear Conditioning

Pretreatment with DPFE (0.1-0.56 mg/kg, i.p.) produced dose-related enhancement in the percentage of freezing behavior during the recording period, significant at the 0.56 mg/kg dose ($F_{3,17}$=4.95 p<0.01; * p<0.01). Bars represent the mean ± s.e.m value for 5-6 rats per group.

Figure 11 DPFE produced dose-dependent reversal of hyperlocomotion in NR1 knockdown mice

A) Mice were administered vehicle or a 30 or 56.6 mg/kg i.p. dose of test compound and placed in the open-field chambers where locomotor activity was monitored for 120 min. DPFE at both doses produced a significant reversal of hyperlocomotion in -/- mice. Wildtype treatment groups did not differ significantly from wildtype vehicle groups. Data are expressed as mean ± s.e.m. of the number of beam breaks/ 5 min; error bars not shown lie within the dimensions of the symbol (n = 6-12 per dose). * denotes p < 0.05 vs. vehicle, Dunnett's test. B) NR1 knockdown mice have significantly impaired performance in the Y maze task compared with littermates. Administration of DPFE (10 mg/kg) did not significantly restore performance of these animals. Data are expressed as mean ± s.e.m %SAP of n=10-13 mice. * denotes p<0.05 vs. vehicle, unpaired T test. C) NR1 knockdown mice have significantly impaired social interactions compared with

littermates. Administration of DPFE (10 mg/kg) did not significantly restore performance of these animals. Data are expressed as mean ± s.e.m of time spent investigating of n=10-13 mice.

Figure 12 In vivo microdialysis in the nucleus accumbens and prefrontal cortex Sprague-Dawley rats were orally administered DPFE at dose 0 (vehicle: ●, n=11), 10 (▼, n=12), 30 (◆, n=13) and 100 (▲, n=9) mg/kg in 20% HPBCD + Tween. Norepinehrine (top row), dopamine (middle row) and serotonin (bottom row) levels were determined from brain dialysates collected in 30 min samples sampled from nucleus accumbens (left column) and prefrontal cortex (right column). * denotes $p<0.05$ vs. vehicle, ANOVA of AUC. Data are expressed as median ± s.e.m. of percentage change of mean individual baseline.

Figure 13 Effects of DPFE on sleep/wake architecture of rats The impact of oral administration of vehicle 20% HPBCD + Tween (black) or DPFE: 10 mg/kg (green); 30 mg/kg (blue); 100 mg/kg (red) with n=8 for each treatment condition during the light phase on time spent in six different sleep-wake states (A-F). Line graphs indicate state amounts expressed as percentage of time spent in state (Y-axis) for consecutive 30 min periods over 20 h post administration (x-axis); inset bar graphs indicate mean±s.e.m time (min) spent in state during first 4 h after administration. * indicates significantly different to vehicle ($p<0.05$), Wilcoxon-Mann-Whitney rank sum test.

Figure 14 Effect of DPFE on pharmaco-electroencephalographic (pEEG) oscillations

Effects of acute oral administration of vehicle (20% HPBCD + Tween: row A), 10 mg/kg (row B), 30 mg/kg (row C) or 100 mg/kg (row D) of DPFE on pEEG relative spectral power in the frontal (left panels) and occipital (right panels) cortical regions in rats (n=8 for each treatment group). Only effects on left hemispheric recordings are shown as no clear differences were detected compared to the contralateral (right hemisphere) traces. Bar charts indicate average percent change from baseline for each EEG spectral band for 8 consecutive 15 min post administration periods. Where δ:1.0-4.0 Hz; θ1: 4.0-6.5 Hz; θ2:6.5-8.0 Hz; α1:8.0-11.0 Hz; α2: 1.0-14.0 Hz; β1: 14.0-18.0 Hz; β2: 18.0-32.0 Hz; γ1: 32.0-48.0 Hz; γ2: 52.0-100 Hz. Values exceeding the 20% change line may be considered significantly different from vehicle ($p<0.05$).

Tables

Table 1: Summary of in vitro potency, affinity and cooperativity parameters for *N*-aryl piperazine PAMs.

	$mGlu_5$-low (Ca^{2+})					$mGlu_5$-high (Ca^{2+})		$mGlu_5$-low (pERK1/2)	
	pEC_{50}[a]	pK_B[b,c]	$log\alpha\beta$[b,c]	pK_B[b,d]	$log\beta$[d]	pK_B[b,d]	$log\beta$[d]	pK_B[b,d]	$log\beta$[d]
DPFE	6.92±0.15 (0.12 μM)	5.32±0.08 (4.8 μM)	1.12±0.11	5.33±0.07 (4.7 μM)	1.14±0.05	5.99±0.12 (1.0 μM)	0.94±0.09	6.87±0.09 (135 nM)	0.12±0.02
VU0364289	6.35±0.12[e] (0.45 μM)	*5.18*[#] *(6.6 μM)*	*0.97*[#]	*5.22*[#] *(6.0 μM)*	*0.90*[#]	*5.83*[#] *(1.5 μM)*	*0.78*[#]	*6.29*[#] *(513 nM)*	*0.16*[#]

[#] data from Gregory et al., 2012 and are provided here for the benefit of comparison.
[a] negative logarithm of the EC_{50}
[b] modulator affinity and cooperativity estimates derived using equation 2, where a composite cooperativity parameter ($log\alpha\beta$) is derived
c negative logarithm of the allosteric modulator equilibrium dissociation constant.
[d] modulator affinity and efficacy cooperativity (β) estimate derived using equation 1, with the assumption that α=1.
[e] VU0364289 potency previously reported in Gregory et al., 2012

Table 2: Effect of mutations on potentiation of glutamate-mediated Ca^{++} mobilization by allosteric modulators.

Data represent mean ± s.e.m of at least four independent experiments performed in duplicate.

	Fold increase in glutamate pEC_{50} in presence of 3 µM PAM			
	CPPHA	VU29	DPFE	VU0364289
$mGlu_5$-wt	3.2±0.1	6.1±1.4	7.7±0.8	4.2±0.7
F585I	1.2±0.1*	11.2±4.8	8.8±2.1	5.6±1.3
A809V	2.8±0.4	2.0±0.3*	2.6±0.2*	1.3±0.1*

* denotes significantly different to $mGlu_5$-wt value, $p<0.05$, one-way ANOVA, Dunnett's post-test.

Table 3 Summary of in vitro and in vivo pharmacokinetic parameters

	VU0364289	DPFE
Cmax (ng/mL)	1280	1093
Tmax (hr)	0.25	0.25
Plasma protein binding	94% (h); 90% (r)	97% (h); 96% (r)
Rat *Fu* (Free fraction)	0.10	0.04

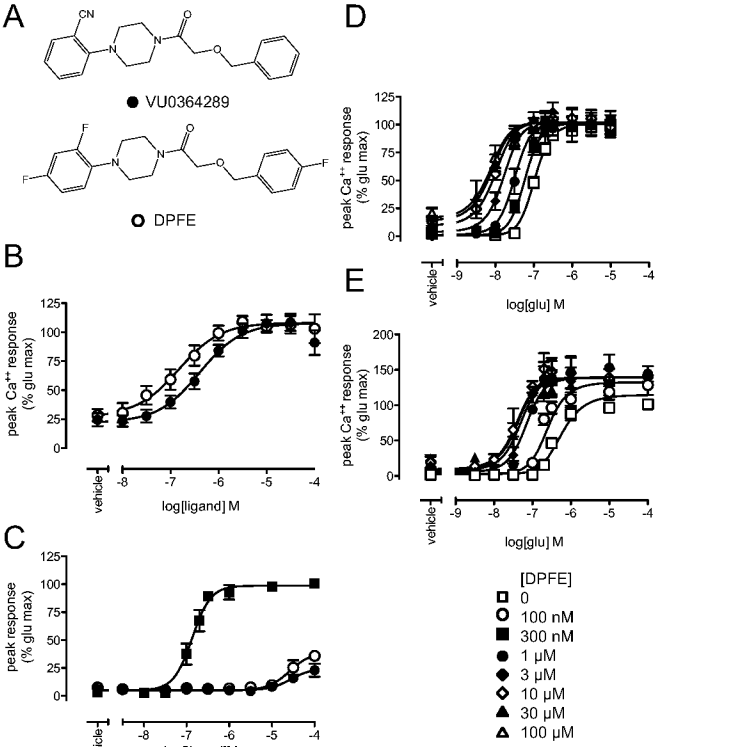
A
CN
VU0364289
F
F
F
DPFE
B
peak Ca++ response (% glu max)
vehicle
log[ligand] M
C
peak response (% glu max)
vehicle
log[ligand]M
D
peak Ca++ response (% glu max)
vehicle
log[glu] M
E
peak Ca++ response (% glu max)
vehicle
log[glu] M
[DPFE]
0
100 nM
300 nM
1 µM
3 µM
10 µM
30 µM
100 µM

Figure 1

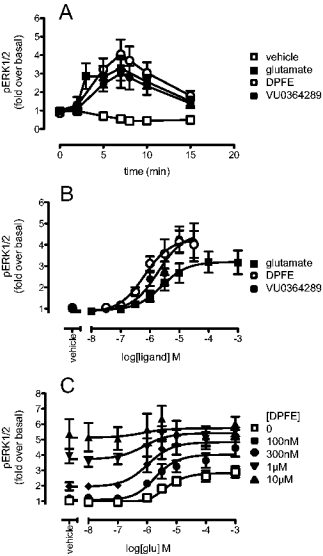
A
pERK1/2
(fold over basal)
vehicle
glutamate
DPFE
VU0364289
time (min)
B
pERK1/2
(fold over basal)
glutamate
DPFE
VU0364289
vehicle
log[ligand] M
C
pERK1/2
(fold over basal)
[DPFE]
0
100nM
300nM
1μM
10μM
vehicle
log[glu] M

Figure 2

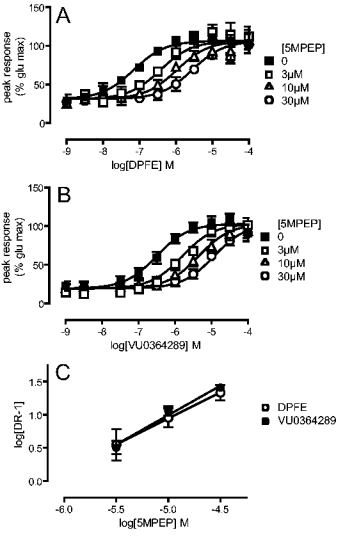
A
peak response
(% glu max)
150
100
50
0
-9
-8
-7
-6
-5
-4
log[DPFE] M
[5MPEP]
0
3μM
10μM
30μM
B
peak response
(% glu max)
150
100
50
0
-9
-8
-7
-6
-5
-4
log[VU0364289] M
[5MPEP]
0
3μM
10μM
30μM
C
log[DR-1]
1.5
1.0
0.5
0.0
-6.0
-5.5
-5.0
-4.5
log[5MPEP] M
DPFE
VU0364289

Figure 3

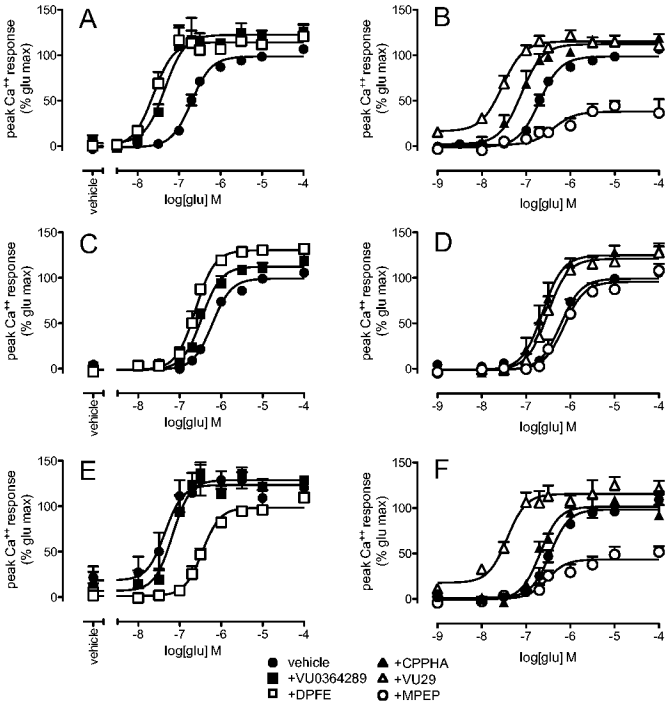
A
B
C
D
E
F
peak Ca++ response (% glu max)
log[glu] M
vehicle
vehicle
+VU0364289
+DPFE
+CPPHA
+VU29
+MPEP

Figure 4

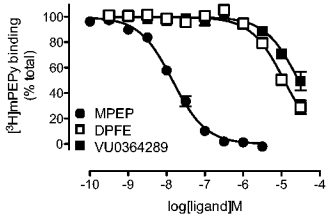
[3H]mPEPy binding
(% total)
100
80
60
40
20
0
MPEP
DPFE
VU0364289
-10
-9
-8
-7
-6
-5
-4
log[ligand]M

Figure 5

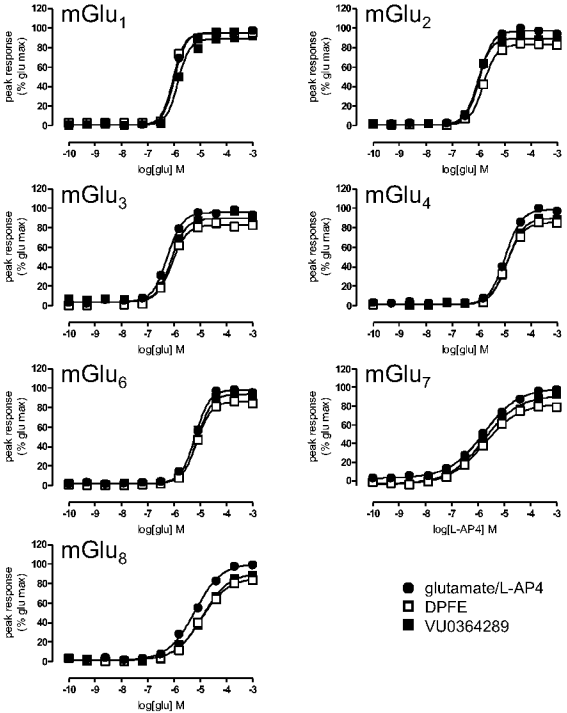
mGlu1
mGlu2
mGlu3
mGlu4
mGlu6
mGlu7
mGlu8
peak response (% glu max)
log[glu] M
log[L-AP4] M
glutamate/L-AP4
DPFE
VU0364289

Figure 6

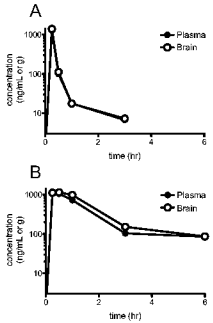
A
Plasma
Brain
concentration (ng/mL or g)
1000
100
10
0
2
4
6
time (hr)
B
Plasma
Brain
concentration (ng/mL or g)
1000
100
10
0
2
4
6
time (hr)

Figure 7

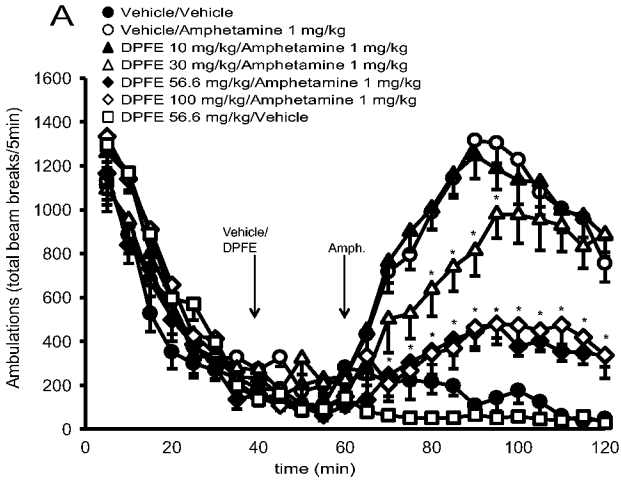
A
Vehicle/Vehicle
Vehicle/Amphetamine 1 mg/kg
DPFE 10 mg/kg/Amphetamine 1 mg/kg
DPFE 30 mg/kg/Amphetamine 1 mg/kg
DPFE 56.6 mg/kg/Amphetamine 1 mg/kg
DPFE 100 mg/kg/Amphetamine 1 mg/kg
DPFE 56.6 mg/kg/Vehicle
Vehicle/
DPFE
Amph.
Ambulations (total beam breaks/5min)
time (min)
0
200
400
600
800
1000
1200
1400
1600
0
20
40
60
80
100
120

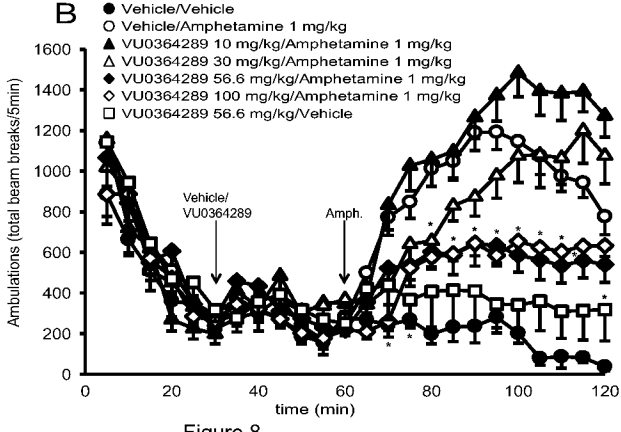
B
Vehicle/Vehicle
Vehicle/Amphetamine 1 mg/kg
VU0364289 10 mg/kg/Amphetamine 1 mg/kg
VU0364289 30 mg/kg/Amphetamine 1 mg/kg
VU0364289 56.6 mg/kg/Amphetamine 1 mg/kg
VU0364289 100 mg/kg/Amphetamine 1 mg/kg
VU0364289 56.6 mg/kg/Vehicle
Vehicle/
VU0364289
Amph.
Ambulations (total beam breaks/5min)
time (min)
0
200
400
600
800
1000
1200
1400
1600
0
20
40
60
80
100
120

Figure 8

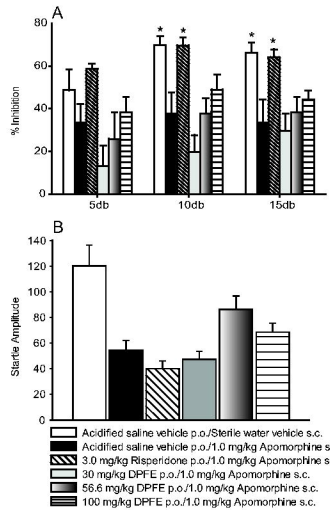
A
% Inhibition
80
60
40
20
0
5db
10db
15db
B
Startle Amplitude
140
120
100
80
60
40
20
0
Acidified saline vehicle p.o./Sterile water vehicle s.c.
Acidified saline vehicle p.o./1.0 mg/kg Apomorphine s.c.
3.0 mg/kg Risperidone p.o./1.0 mg/kg Apomorphine s.c.
30 mg/kg DPFE p.o./1.0 mg/kg Apomorphine s.c.
56.6 mg/kg DPFE p.o./1.0 mg/kg Apomorphine s.c.
100 mg/kg DPFE p.o./1.0 mg/kg Apomorphine s.c.

Figure 9

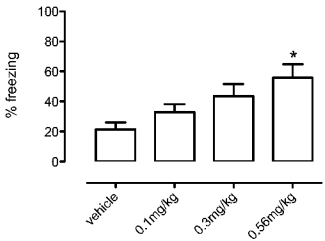

Figure 10

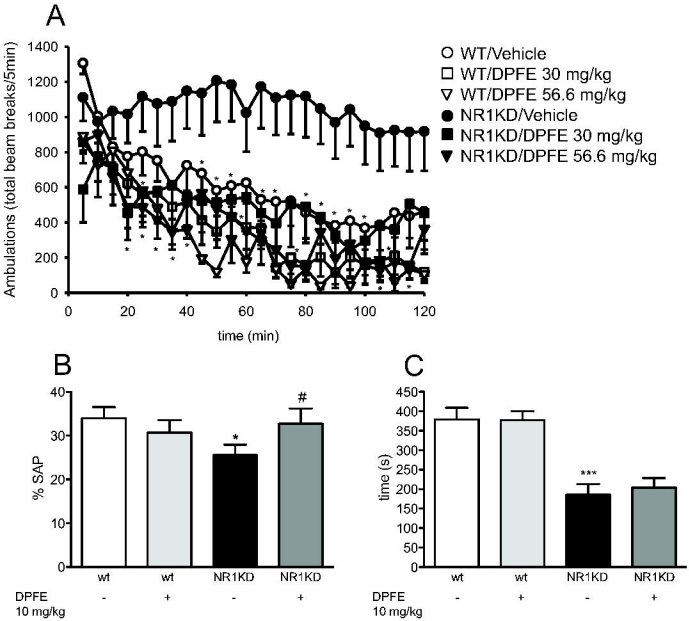
A
Ambulations (total beam breaks/5min)
1400
1200
1000
800
600
400
200
0
0
20
40
60
80
100
120
time (min)
WT/Vehicle
WT/DPFE 30 mg/kg
WT/DPFE 56.6 mg/kg
NR1KD/Vehicle
NR1KD/DPFE 30 mg/kg
NR1KD/DPFE 56.6 mg/kg
B
% SAP
40
30
20
10
0
*
#
wt
wt
NR1KD
NR1KD
DPFE
10 mg/kg
-
+
-
+
C
time (s)
450
400
350
300
250
200
150
100
50
0
***
wt
wt
NR1KD
NR1KD
DPFE
10 mg/kg
-
+
-
+

Figure 11

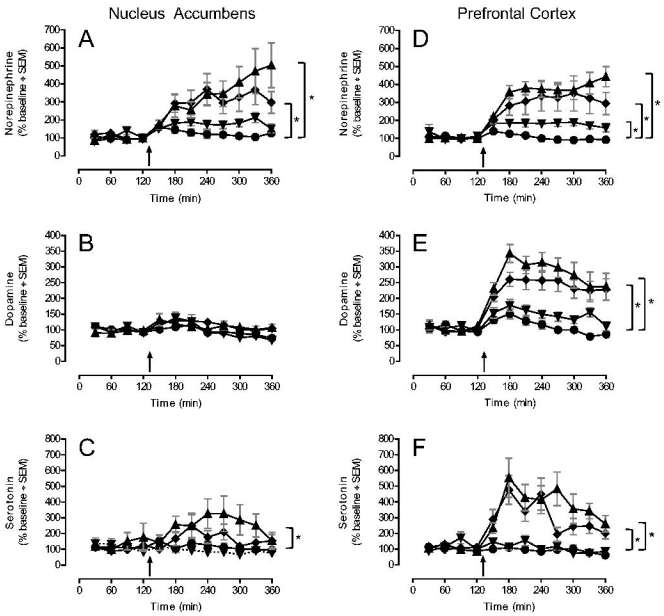
Nucleus Accumbens
Prefrontal Cortex
A
B
C
D
E
F
Norepinephrine (% baseline + SEM)
Dopamine (% baseline + SEM)
Serotonin (% baseline + SEM)
Time (min)
0
60
120
180
240
300
360
*

Figure 12

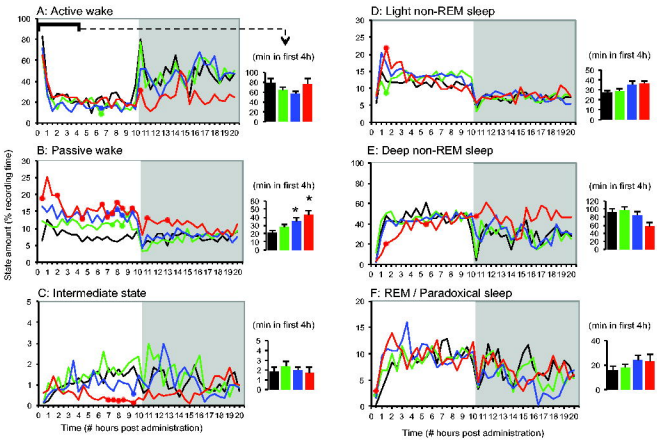
A: Active wake
B: Passive wake
C: Intermediate state
D: Light non-REM sleep
E: Deep non-REM sleep
F: REM / Paradoxical sleep
(min in first 4h)
State amount (% recording time)
Time (# hours post administration)

Figure 13

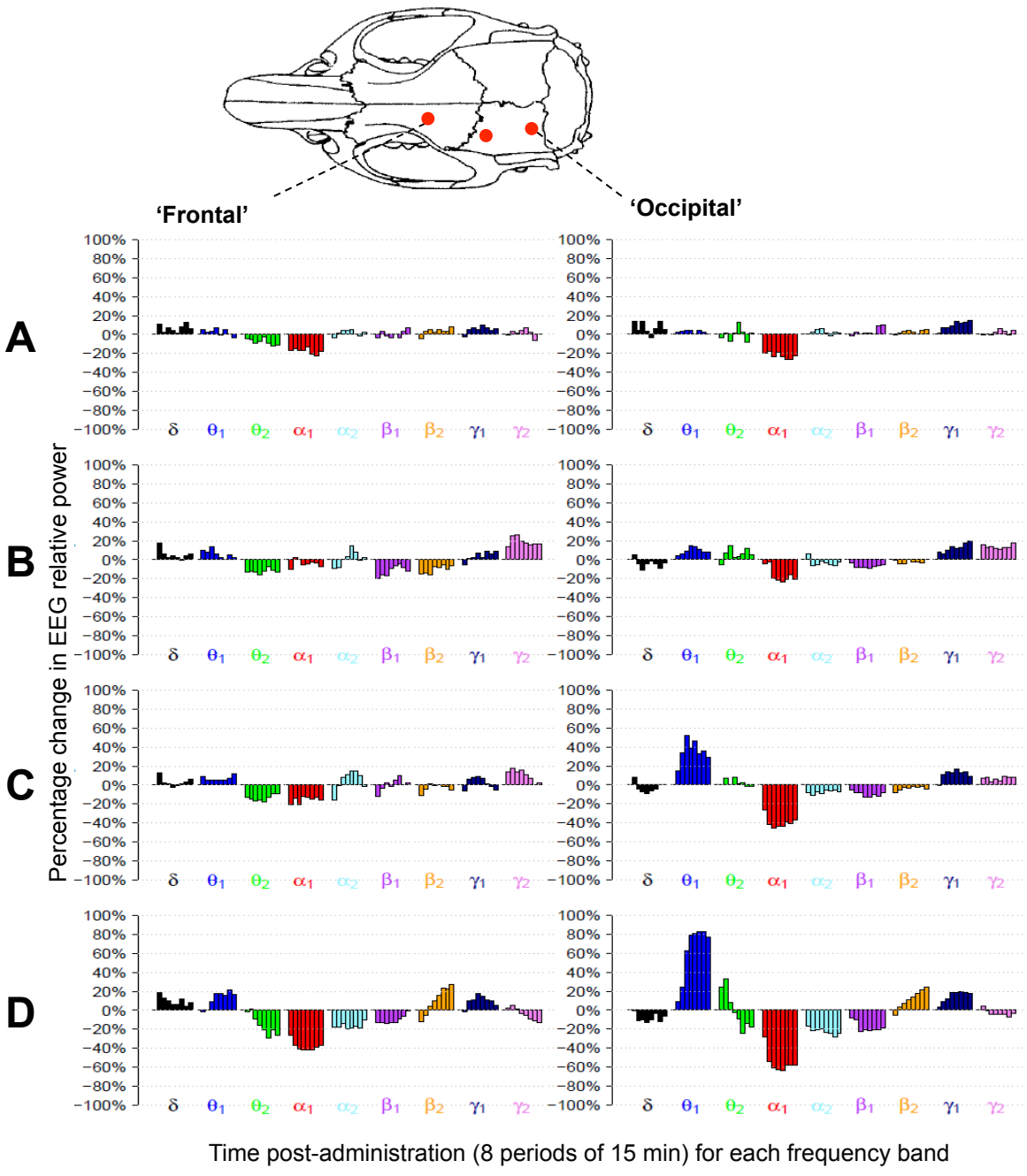
'Frontal'
'Occipital'
A
B
C
D
Percentage change in EEG relative power
100%
80%
60%
40%
20%
0%
−20%
−40%
−60%
−80%
−100%
δ θ1 θ2 α1 α2 β1 β2 γ1 γ2
Time post-administration (8 periods of 15 min) for each frequency band

Figure 14